Physica B 406 (2011) 2931–2947

Contents lists available at ScienceDirect

Physica B

journal homepage: www.elsevier.com/locate/physb

Molecular dynamics simulation of interfaces and surfaces in structures derived from α-quartz- and ZSM-5 crystallites

A. Brinkmann, F. Langer, F. Scholler, Z. Shan, J. Wilmers, Y. Zhao, C. Oligschleger *

Department of Applied Science, Bonn-Rhine-Sieg University of Applied Sciences, Germany

ARTICLE INFO

Article history:
Received 30 July 2010
Received in revised form
8 January 2011
Accepted 4 February 2011
Available online 22 April 2011

Keywords:
Molecular dynamics
Nano-systems

ABSTRACT

We investigated structures derived from α-quartz- and ZSM-5-crystallites in different orientations and combinations. Gaps are introduced into the configurations in order to produce surfaces. However, interfaces can be formed by coalescence of surfaces. The structural and thermal properties of the thus generated interfaces and of the remaining surfaces are qualitatively discussed. Applying different sizes of the gaps between the structures allowed the monitoring of structural changes, partial pair-correlation functions and bond-angle distributions. Furthermore, we discuss the influence of the thermal or temperature distribution in the thus constructed materials. We report about the qualitative differences using both constant temperatures and temperature gradients.

1. Introduction

In nano-technology the influences of surface effects, interfaces, borders and boundaries play a crucial role for the understanding of material properties important in chemistry and physics. In biology and life science the behaviour of micelles and vesicles is also strongly dominated by surfaces. Furthermore, the properties of surfaces or interfaces are important for the development of nano-devices in technical applications. Especially the design of integrated circuits is dominated by the generation of thin films and nano-wires where the mean free paths of the phonons are restricted by the size of the nano-devices, and thermal transport through interfaces and barriers is strongly affected by the Kapitza resistance [1]. This is a field of both experimental and theoretical research [2]. The influence of nano-particles on tensile strength, thermal and mechanical properties of (nano-)composites is investigated to produce tailoured materials [3]. For a comprehensive review and further reading we address to Ref. [4]. Nucleation and growth processes of nano-scaled silica have been investigated experimentally for more than a decade [5], especially the reactions and thermodynamic analysis of nano-particles are in the focus of technical approaches, where coalescence and sintering influence catalytic properties and diffusivity of nano-structures [6]. On the other hand molecular dynamics simulations of nano-particles study their thermodynamic properties and the high temperature reactivity [7,8]. One aim of our simulations is to investigate structural properties and their changes in materials with different interfaces or surfaces depending on gap-size and composition. Another focus is laid on the temperature and energy distributions in nano-scaled systems caused by structural defects like gaps, boundaries and borders. The understanding of heat resistance and energy transfer in materials with boundaries between crystallites is of importance for the design of devices on nano-meter scale, since their functionality and life-time are influenced by temperature, temperature differences and energy barriers. Especially, if devices are exposed to situations with temperature changes both the heat flow and the material's heat resistivity will become central properties which influence the behaviour of the materials. Other important applications beside the construction of electrical devices are the understanding of the temperature drops in micro- or nano-sized (metallic) contacts used in cryogenic instruments [9] or the study of temperature relaxations at interfaces of hetero-structures, e.g. thin (Bi-)films deposited on silicon [10]. Therefore, we perform molecular dynamics simulations at both constant temperatures and temperature gradients.

The investigation of nano-materials is a field of continuous improvement for both practical applications and basic research [11–13]. The thermodynamic and kinetic properties of materials are not only ruled by, e.g. low-frequency modes and the so-called Bose-peak which is shown to be dependent on the degree of amorphization [14]. The role played by the structures themselves is also important, since the structure–property relations are essential for further insights. More global aspects, e.g. the concept of energy landscape [15,16], use thermodynamic properties of crystalline structures in order to predict novel materials. The focus of our investigations is also laid on the energetic development of the system under consideration, i.e. the relaxation of the

* Corresponding author. Tel.: +49 2241 865 562; fax: +49 2241 865 8562.
E-mail address: christina.oligschleger@h-brs.de (C. Oligschleger).

0921-4526/$ - see front matter © 2011 Elsevier B.V. All rights reserved.
doi:10.1016/j.physb.2011.02.074

structures [17–20]. Other groups report on dynamical processes [21–25], aging [26–28] and mode-analysis [29–32] in different amorphous systems. For the simulations we use a classical molecular dynamics approach which is a state of the art method for more than three decades [33–36], which is also recently used for the study of different surface effects [37–40]. Interfaces between crystals and melts are also subject of numerical investigations elucidating both kinetic behaviour and free energies [41–43]. Nevertheless, one should have in mind that in nano-systems the physics is governed and dominated by quantum effects which are not considered in this type of simulation. So, electronic contributions are neglected and only atomic/vibronic behaviour is taken into account. However, since the system sizes which we consider exceed 1000 atoms, our simulations could not easily be transferred to quantum-mechanical calculations, however these would be helpful. The article is organized as follows: in the next section we give an overview over the models and the potential mimicking the atomic interactions, used throughout the simulations, and describe computational details. The results of structural and thermal properties are presented in the third section, followed by a discussion. In the final section we summarize and give conclusive remarks.

2. Models, potential and computational details

For our investigations we used models based on silicate-structures—as α-quartz-modification, and zeolite-structures—as silicalite ZSM-5-form. In order to simulate the influence of grain boundaries, interfaces and structural gaps on static and dynamic properties, we constructed crystallites and introduced gaps (e.g. parallel to the *y*–*z*-plane), i.e. we divided the structures into two parts and separated them by distances ranging from 0 up to 10 Å. We would like to emphasize that the MD-calculations are done *in vacuo*, i.e. there is no substrate on which the configurations are grown or otherwise deposited. So our structures are not fixed by a larger base which could act as a medium contributing to the heat transport or influencing the thermal properties. We investigated three models: α-quartz−α-quartz, ZSM-5–ZSM-5 and ZSM-5−α-quartz. In detail we built an α-quartz-crystallite comprising 2160 atoms in a box with side-lengths of $a=39.28$ Å, $b=25.51$ Å and $c=27.00$ Å, respectively. A gap along the *x*-direction is constructed by separating the quartz-structure in the middle (e.g. of the *x*-axis) and shifting the two parts 0, 0.4, 2.0, 2.8, 4.0 and 8.0 Å apart in such a way that gaps of respective size are created and the box-length in *x*-direction is increased from 39.28 to 39.68, 41.28, 42.08, 43.28, and 47.28 Å.

To reduce the influence of surface effects caused by the finite size of the structures, periodic boundary conditions are established, i.e. only one gap is established in the centre of the structure, since due to periodic boundary conditions the surfaces of the structure will interact with the opposite ones and are connected via bonds. The second type of system comprises 1152 atoms of a ZSM-5-crystallite with $a=40.04$ Å, $b=19.90$ Å and $c=26.77$ Å being its lateral dimensions. We introduce gaps of size 0, 0.4, 2.0, 2.8, 4.0 and 8.0 Å along the *x*-direction by cutting the configuration perpendicular to the *y*–*z*-plane and separating the two sub-structures to the respective distances. Again we apply periodic boundary conditions to embed the crystallite in a crystalline surrounding. The third type of configurations which are under investigation comprise both an α-quartz and a ZSM-5-structure. In contrast to the previous models we have a mismatch between the two parts from the beginning of the simulation, i.e. we have to introduce two gaps instead of one. The first gap is found in the centre where the structures are put together. The second gap is due to periodic boundary conditions since the configurations will not match. One mixed model is generated from 1296 atoms (576 atoms from a ZSM-5-structure and 720 atoms building an α-quartz-configuration). The structures are aligned in *y*-direction and the gaps in the centre are 0.5, 1.0, 5.0, and 10.0 Å and by applying periodic boundary conditions a gap of 1.0 Å is introduced in the *y*-direction at the boundary. The dimensions of the combined crystals are $a=20.02$ Å and $c=27.00$ Å, and due to the established gaps the dimension *b* in the *y*-direction will have the values $b=37.56$, 38.06, 42.06 and $b=47.06$ Å, respectively. Another alignment comprising 4248 atoms is realized using an α-quartz of 2520 atoms and 1728 atoms forming a ZSM-5-crystal. The two crystallites are aligned along the *x*-direction. In this mixed system we constructed six starting configurations and established two gaps in each with sizes 0.1/0.2, 0.5/1.0, 1.0/2.0, 1.5/3.0, 2.0/4.0 and 4.0/8.0 Å, the first value is the size of the gap in the centre and the second number gives the width of the second gap at the boundary, respectively. The lateral dimensions in the *y*- and *z*-directions are $b=59.70$ Å and $c=27.00$ Å, in the *x*-direction the crystallites *a* stretches from $a=39.57$, 40.77, 42.27, 43.77, 45.27 to 51.27 Å.

All the above described structures are based on SiO_2-configurations. For the simulations of the SiO_2-structures we used the potential proposed and fitted by Vashishta et al. [44]. The potential consists of two-body (including long-range Coulomb interactions, terms describing damped dispersion and a general potential type) and three-body terms (described by Stillinger–Weber potentials [45,46]):

$$V=\sum_{i=1,j>i}^{N} V_2(r_{ij})+\sum_{i=1,j>i,k>j}^{N} V_3(r_i,r_j,r_k) \tag{1}$$

in order to reproduce structural and dynamical properties of both crystalline and amorphous phases. The two-particle interaction contains a long-range Coulomb part that we treat with Ewald summation [47,48], and includes terms accounting for the steric repulsion of the particles and for the polarizability of the atoms.

The two-particle potential is given by

$$V_2(r)=\frac{Z_iZ_j}{r}+\frac{H_{ij}}{r^{\eta_{ij}}}-\frac{\frac{1}{2}(\alpha_iZ_j^2+\alpha_jZ_i^2)}{r^4}\exp(-r/r_{4s}) \tag{2}$$

Z_i is the effective charge and α_i is the electronic polarizability of atom *i*, and H_{ij} and η_{ij} describe the steric repulsion of atoms *i* and *j*. The three-body-interaction is relevant only for triplets Si–O–Si and O–Si–O, the other possible combinations (Si–O–O, O–Si–Si, O–O–O, and Si–Si–Si) are neglected. The three-particle-term favours the development of the tetrahedral angle at the silicon and of an angle $\Theta_0\approx 140^\circ$ at the corner sharing oxygen. The functional form of the three-particle-term is

$$V_3(r)=B_{ijk}\exp\left(\frac{1}{r_{ij}-r_0}+\frac{1}{r_{ik}-r_0}\right)(\cos(\Theta_{ijk})-\cos(\Theta_0))^2,\quad r_{ij},r_{ik}<r_0$$

$$V_3(r)=0,\quad r_{ij},r_{ik}\geq r_0 \tag{3}$$

All parameters are given in Ref. [44]. The applicability of this potential to surfaces, interfaces or dynamics of structural defects (e.g. crack propagation) of both crystalline silica conformations and amorphous silica have been shown in several studies [49–52] in which the coalescence of surfaces and cavities have been investigated.

With molecular dynamics (MD) one can simulate a variety of complex structures [53–57]. In order to determine structural, dynamic and thermodynamic quantities, one typically explores correlation functions, e.g. determination of the van Hove correlation gives insight into the radial distribution of atomic distances, and the calculation of the velocity autocorrelation [58] or displacement autocorrelation [59] reveals the vibrational spectrum of configurations. After initially introducing surfaces and gaps of

different sizes into the system, the structure is monitored for typically 50 000 molecular dynamics time steps (each 1.0 or 2.0 fs) with a velocity Verlet integration scheme at a temperature of 600 K, i.e. well below the glass transition temperature. For several structures we performed MD-runs up to 5 sns in order to test the stability and equilibration of the systems. We applied periodic boundary conditions to reduce surface effects caused by the system size. The starting volume is conserved within the simulation and we monitored the virial of the configuration to account for internal pressure. Nevertheless, one should have in mind that due to the fact that the simulations are performed *in vacuo* and that the gaps lead to "free" volume or additional space which gives rise to relaxation processes.

The additional space also causes a decrease in the density ρ. In order to account for the structural homogeneity of the systems, we calculate the standard deviation of the density within a configuration. To do so, we split the structures into 125 subcubicles (small enough to give a reasonable statistics and large enough to contain an average number of at least 10 atoms) for which we calculated the densities and the respective relative standard deviation $\Delta\rho/\rho$. One can imagine that the existence of voids, pores, channels and gaps on one hand, and interfaces and different structural species on the other hand increases the standard deviation of the mass density. Another structural property which clearly exhibits the crystalline or disordered status of matter is the so-called total pair-correlation function $g(r)$:

$$g(r) = \left\langle \frac{n(r)}{4\pi r^2 \rho_N \Delta r} \right\rangle \tag{4}$$

with $n(r)$ being the number of atoms at a distance r in a sphere with thickness Δr around a reference atom, ρ_N is the number density of atoms in the system and $\langle\ \rangle$ stands for the averaging over configurations which are calculated throughout the molecular dynamics simulations. In our simulation we mainly focus on the partial pair-correlation functions $g_{\alpha\beta}$:

$$g_{\alpha\beta}(r) = \left\langle \frac{n_{\alpha\beta}(r)}{4\pi r^2 \rho_\beta \Delta r} \right\rangle \tag{5}$$

where $n_{\alpha\beta}$ is the number of species β in a shell of thickness Δr and radius r around atom type α and ρ_β is the number density of atom β with $\alpha,\beta =$ Si,O. Measuring the bond angles reveals the short-range structure of the configuration, i.e. the building units and their connectivity. Since our systems consist of two atom-types we have six types of bond angles Θ_{ABC}, with A–B–C being Si–O–Si, O–Si–O, Si–Si–O, O–O–Si, Si–Si–Si, and O–O–O, which are calculated using the following equation:

$$\Theta_{ABC} = \arccos\left(\frac{\mathbf{r}_{BA}\mathbf{r}_{BC}}{|\mathbf{r}_{BA}||\mathbf{r}_{BC}|}\right) \tag{6}$$

with $\mathbf{r}_{BA}$ and $\mathbf{r}_{BC}$ being the vectors between the atoms A and B or C and B, respectively and with B being the central atom from which the angle is measured to the adjacent atoms A and C. From previous simulations of both α-quartz and ZSM-5-type of zeolite the distances of the neighbouring atoms are well known and we use as cut-off-distances for $r_{SiO}=2.2$ Å, $r_{OO}=3.0$ Å and $r_{SiSi}=3.6$ Å, these values coincide with first minima of the partial pair-correlation functions [60,61].

In order to measure the amorphicity of the structures, we introduce the distance between the starting reference phase and the optimized configurations as quantifiable observable. The atomic shifts are measured from the squared displacements:

$$\Delta R^2 = \sum_n (\mathbf{R}_n^i - \mathbf{R}_n)^2 \tag{7}$$

where $\mathbf{R}_n^i$ is the position vector of atom n in its position in minimum i of the potential energy surface and $\mathbf{R}_n$ is the position of atom n in the reference configuration. The total displacement R which accounts for a structural change is given by $R=\sqrt{\Delta R^2}$ and measured in Å.

The temperatures in the simulations are determined from the velocities of the atoms. In canonical simulations (NVT-ensemble) the velocities of the atoms are rescaled each 100 time-steps in order to keep the temperature constant. In runs where temperature gradients are applied, the temperatures of two layers (comprising 10% of atoms each) are fixed at 300 and 900 K, respectively, by rescaling the atomic velocities at each time-step, all other atoms are allowed to evolve according to Newton's law. The spatial distribution of the temperature is calculated by dividing the volume into 10 sectors of equal spatial size along the alignment of the crystalline structure, i.e. there could be sector comprising only a few atoms of the structure or even no atom, since these sectors or layers are located either close to the gap or completely in the gap. Furthermore, due to atomic shifts the number of atoms comprising these layers will fluctuate, and consequently the temperature of the layers will fluctuate, respectively.

3. Results

The investigations of the influence of boundaries and gaps on structural properties, i.e. pair-correlation functions and bond-angle distributions, and on temperature distributions are performed for three different types of systems. We constructed an α-quartz-crystallite on an α-quartz-configuration comprising 2160 atoms aligned in x-direction and separated by 0, 0.4, 2.0, 2.8, 4.0 and 8.0 Å. A second type of structure is investigated by deposing a ZSM-5-structure on another ZSM-5-configuration in x-direction using the same gap-sizes as above. The total structure has a total of 1152 atoms. As a third type of configuration we considered mixed structures, i.e. combinations of α-quartz and ZSM-5-zeolite. In contrast to the systems comprising only one crystalline species, the mixed forms have two gaps. For the mixed configurations we investigated small structures comprising in all 1296 atoms (720 atoms from an α-quartz-crystallite and 576 atoms from a zeolite-structure are aligned in y-direction) with gaps of 0.5/1.0, 1.0/1.0, 5.0/1.0, and 10.0/1.0 Å. The first value gives the size of the central gap and the second number refers to the gap-size due to periodic boundary conditions. A larger system combines an α-quartz-crystallite of 2520 atoms and a ZSM-5-configuration with 1728 atoms and aligns these structures along the x-direction with two gaps of 0.1/0.2, 0.5/1.0, 1.0/2.0, 1.5/3.0, 2.0/4.0 and 4.0/8.0 Å. Again the first values describe the central gap, whereas the second number gives the gap-size at the boundary.

In all three systems a general observation concerning the coalescence of surfaces can be seen from monitoring the trajectories of the atoms. If the distance between the surfaces is small enough, the atoms move towards each other, form new bonds and close the gap. Besides the puzzling individual motions, we monitored the total displacement R as a more general observable. From previous simulations the total atomic displacement is known to be a good quantity for exhibiting (local) relaxations or for revealing the diffusive character of a system. It is also known that the (short-time) fluctuations in R follow from the vibrations underlying the dynamics of the configurations. In Table 1 we summarize informations for all systems under investigation and present the values on the applied gap-sizes, corresponding densities ρ with the relative standard deviations $\Delta\rho/\rho$, the total displacements and averaged atomic shifts for both constant temperature runs and simulations of temperature gradients. Those simulations, in which the systems relax in order to close

Table 1
Total displacements and atomic shifts of all simulations are given for both constant temperature and temperature gradient. In the first column the model-systems and their respective atom numbers are given. In the next column the gap-sizes in the centre of the structures and at the boundary are presented. The third column refers the corresponding densities and the relative standard deviations, followed by the total and atomic displacements for both set-ups, i.e. values for constant temperature and for temperature gradients are given.

Type of system, number of atoms	Gap-size (Å)	ρ (g/cm^2)/$\Delta\rho/\rho$	Constant temperature		Temperature gradient	
			Total shift R (Å)	Atomic shift $\sqrt{R^2/N}$ (Å)	Total shift R (Å)	Atomic shift $\sqrt{R^2/N}$ (Å)
Quartz–quartz, $N=2160$	0.0	2.631/0.101	9.72	0.21	9.98	0.21
	0.4[a]	2.605/0.102	10.34	0.22	10.29	0.22
	2.0[a]	2.505/0.105	35.55	0.76	21.73	0.47
	2.8[a]	2.459/0.099	39.08	0.84	39.10	0.84
	4.0[a]	2.392/0.111	46.05	0.99	46.49	1.00
	8.0	2.192/0.429	21.64	0.47	20.91	0.45
ZSM–ZSM, $N=1152$	0.0	1.780/0.340	14.48	0.43	14.48	0.43
	0.4[a]	1.695/0.347	23.70	0.70	23.70	0.70
	2.0	1.664/0.370	23.70	0.70	25.70	0.76
	2.8	1.618/0.423	38.48	1.13	41.61	1.23
	4.0	1.548/0.527	44.68	1.32	42.99	1.27
	8.0	1.483/0.540	34.68	1.02	32.38	0.95
Quartz–ZSM, $N=1296$	0.5/1.0[b]	2.076/0.319	60.87	1.69	60.26	1.67
	1.0/1.0[b]	1.997/0.350	77.52	2.15	80.04	2.22
	5.0/1.0[a]	1.878/0.332	69.50	1.93	68.89	1.91
	10.0/1.0[a]	1.679/0.439	65.36	1.82	66.41	1.84
Quartz–ZSM, $N=4248$	0.1/0.2[b]	2.195/0.208	48.85	0.75	24.84	0.38
	0.5/1.0[b]	2.130/0.254	83.02	1.27	79.12	1.21
	1.0/2.0[a]	2.055/0.350	100.87	1.55	101.90	1.56
	1.5/3.0[a]	1.984/0.395	110.25	1.69	111.45	1.71
	2.0/4.0[a]	1.919/0.473	123.76	1.90	126.08	1.93
	4.0/8.0[a]	1.694/0.557	172.00	2.64	163.15	2.50

[a] In case of only one gap, an interface is generated, if there are two gaps, the smallest one is closed.
[b] Two gaps are present in the starting structures which are both closed via coalescence of the surfaces.

the gaps, are marked and one can observe an increase of the atomic shifts with decreasing densities (see e.g. the simulations marked with footnote a of the quartz–quartz systems and those of the large quartz–ZSM structures show a linear increase of the atomic shifts with increasing gap-sizes.) This hints towards a combination of the complete displacement into a "diffusive" part (in order to overcome the gap) and a local relaxational part.

At the beginning of the simulation the systems are in non-equilibrium states and therefore, one can observe large fluctuations in all monitored variables during which the systems equilibrate to lower energetic states. This can also be seen in the total displacement, which shows a wave-like behaviour at the beginning of the simulation, followed by the typical small fluctuations. The "first waves"/peaks in R—in connection with the individual trajectories—results from the coalescence of the surfaces. Astonishingly, for all those cases, in which we observed the coalescence of the surfaces, one can see that this coalescence is finished within a few pico-seconds, and is rather independent of both the gap-size and the system-type. However, these motions lead to an "impact" velocity of the surfaces of the order $O(10^2$ m/s). After the coalescences of the surfaces are finished, relaxations—also due to the impacts—take place. Here, the types of these relaxations are not studied in detail and we refer to other publications which in detail describe heterogeneities and non-Gaussianities observed in relaxations [62–64].

3.1. α-Quartz−α-quartz

For the α-quartz−α-quartz-structures comprising 2160 atoms we performed MD-runs at an averaged temperature of 600 K with an observation time of 100 ps. The simulation of interfaces and boundaries is performed by introducing different gap-sizes (0, 0.4, 2.0, 2.8, 4.0 and 8.0 Å), i.e. we split the structure into two parts and separate the two sub-structures, periodic boundary conditions are applied in all directions. In a second modelling route we would like to estimate the influence of temperature gradients by fixing the temperature of two layers at temperatures of 300 and 900 K, respectively. Using Molden [65] we display configurations for different gap-sizes in Fig. 1. On the left side of the figure starting configurations with gap-size 4 Å (top) and 8.0 Å (down) are shown. The right panel gives the resulting configurations after

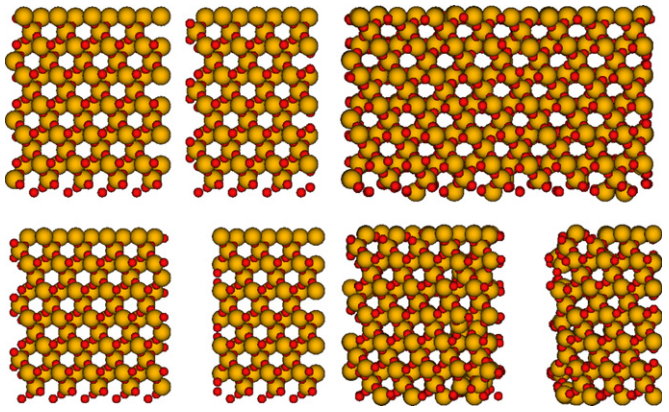

Fig. 1. Left: Starting configurations of the α-quartz−α-quartz-structures comprising 2160 atoms with gaps of 4 Å (top) and 8.0 Å (down) thickness. Yellow (light-grey) and red (dark-grey) spheres represent Si and O atoms, respectively. View is along the [0 0 1] direction. Right: Configurations after a constant temperature run with a total displacement of $\Delta R \approx$ 46 and 22 Å from the starting configuration, respectively. (For interpretation of the references to colour in this figure legend, the reader is referred to the web version of this article.)

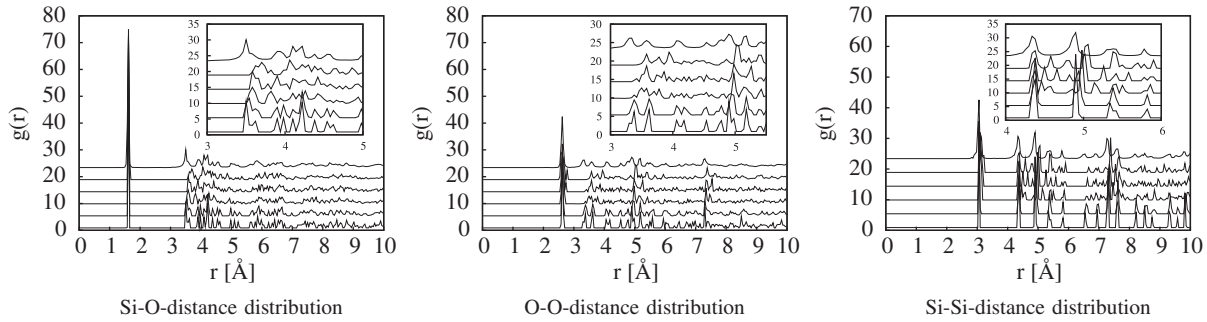

Fig. 2. The partial pair-correlation functions for the α-quartz−α-quartz-structures are shown for the calculations using constant temperature. The lines in each figure correspond to different gap-sizes between the structures: 0, 0.4, 2.0, 2.8, 4.0 and 8.0 Å (bottom-up). The insets are an enlargement of the intermediate regions.

a constant temperature run with the respective displacements from the starting configurations. From the total displacements one can calculate the averaged atomic displacement, for a gap with a size of 4 Å each atom is displaced by 0.99 Å, and for the largest gap-size an atom is on average displaced by 0.47 Å.

From our simulations we find that a starting gap of 4.0 Å at the beginning of the simulation is closed by the coalescence of the two surfaces. This fast global equilibration is performed within few ps and leave most of the observation time of 100 ps for local structural rearrangements.

In the case of a starting gap-size of 8 Å between the two α-quartz-crystallites the observation time is much too short in order to significantly close the gap. At the end of the observation time the surfaces have developed some defects and comprise partially disordered regions. To have a closer look at the structures we calculated the partial pair-correlation functions. In Fig. 2 we show the pair-correlation functions $g(r)$ for the pairs Si–O, O–O and Si–Si, respectively. The simulations were performed at a constant temperature of about 600 K. In each figure the different lines represent the different gap-sizes from 0 Å (bottom) up to 8.0 Å (top), respectively. For the constant temperature runs the insets show the distance-distributions at intermediate ranges.

The Si–O-distance distributions are dominated by the first neighbour peak for all gap-sizes. The inset shows that the first peaks of the Si–O-distances in the intermediate region broaden and are slightly shifted to larger values. However, for the largest gap-size of 8 Å the peaks in the structural intermediate-range order are shifted "back" to the same distances as in the case without a gap. In the O–O-distance distribution the first peak at $r=2.6$ Å broadens with increasing gap-size and a shoulder or a smaller second peak develops. To recognize differences in the structures with different gap-sizes one should have a closer look at the intermediate-range order, here we can see the similarity of those structures which have either no gap or a very small gap. For structures with a medium gap-size (2.0 Å up to 4.0 Å) we observe a shift to higher distances in the intermediate-range order. Only in the case of the largest applied gap (8 Å) the distances are shifted to slightly shorter values and a broadened peak pattern occurs.

Similar to the O–O distribution a small broadening of the first peak in the Si–Si-distances is found with increasing gap-size. At intermediate distances we find sharp peak distributions for gap-sizes up to 0.4 Å, for larger gap-sizes the peaks broaden and additional peaks occur. The crystallinity of the structures can be seen from some peaks, well beyond the next-nearest neighbour distances, which reflect the lattice constants at $a=4.91$ Å and $c=5.4$ Å. The peak at 7.3 Å is the hypotenuse of the lattice constants a and c, the hexagonal symmetry of α-quartz can be identified in the peak at 8.5 Å ($\approx 2\cdot a\cdot\cos(30^\circ)$). The peak at 9.8 Å is the double of the lattice constant a. Since the silicon atoms are the "back-bone" of the network, the above mentioned distances are clearly present in the partial pair-correlation of the Si–Si distribution for gap-sizes up to to 0.4 Å. For larger gap-sizes these peaks broaden or split into several additional peaks. These peaks (caused by the crystalline structure) also show up in the O-O-distances, however these peaks exhibit the greater flexibility of the oxygens in comparison to the silicon atoms since the intensity of the peaks corresponding to the lattice constants are reduced compared to the Si–Si-distances, and a broadening and splitting of the lattice-peaks can already been observed for the smallest gap-size. Since the results of the partial pair-correlation function found for the simulation of temperature gradient are very similar to those determined for constant temperature runs, we do not present the graphs.

The bond-angle distributions shown in Fig. 3) result from constant temperature runs. Our findings exhibit clearly the tetrahedral short-range structure. However, all possible bond angles show both a slight broadening of the peaks and shifting of the peak positions with increasing gap-size (from bottom to top the gap-sizes are 0, 0.4, 2.0, 2.8, 4.0 and 8.0 Å). The simulations of the structures subjected to temperature gradients show nearly the same angle distributions, and therefore, the bond-angle distributions from runs using temperature gradients are not shown.

In detail we observe the O–Si–O distribution to have a peak-position at 109° which is a strong hint towards the existence of only slightly distorted tetrahedrons as basic structural unit, shoulders and side peaks occur for gap-sizes larger than 2.8 Å, this result correlates with the broadening of the first peak of the O–O-distance in Fig. 2. The Si–O–Si distribution has a peak-position at 145° which is shifted to 155° for gap-sizes from 0.4 to 4.0 Å. In the case of a gap-size of 8 Å the peak-position is shifted (back) to the position at 140°. Since this distribution is much smaller compared to the one found in silica glasses [60] the overall order of the network is conserved. In the Si–Si–O angle distribution the peak around 20° stems from two silicons belonging to the same oxygen. This peak is directly connected to the Si–O–Si distribution, and similar to this distribution we observe a slight shift of this peak. If the oxygen is not the bridging atom between the two silicons and is only neighbour to the ad-atom the angle is between 90° and 130°. The O–O–Si angle distribution shows a peak at 35° which is caused by oxygens belonging to the same tetrahedron, this result is in direct connection to the sharp tetrahedral peak found in the O–Si–O angle distribution. This peak is stable for all gap-sizes which is—again—a strong hint towards the stability of the tetrahedrons as building units. Since the central oxygen bridges two tetrahedrons, the peak distribution between 110° and 170° stems from the fact that the second O belongs to the (via corner-sharing by the first O) bridged tetrahedron (another Si). For the Si–Si–Si angle we find relatively sharp peaks between 90° and 150° which will broaden with increasing gap-sizes. The strong peak at 60° in the O–O–O angle distribution (for all gap-sizes) is caused by three O which belong to the same

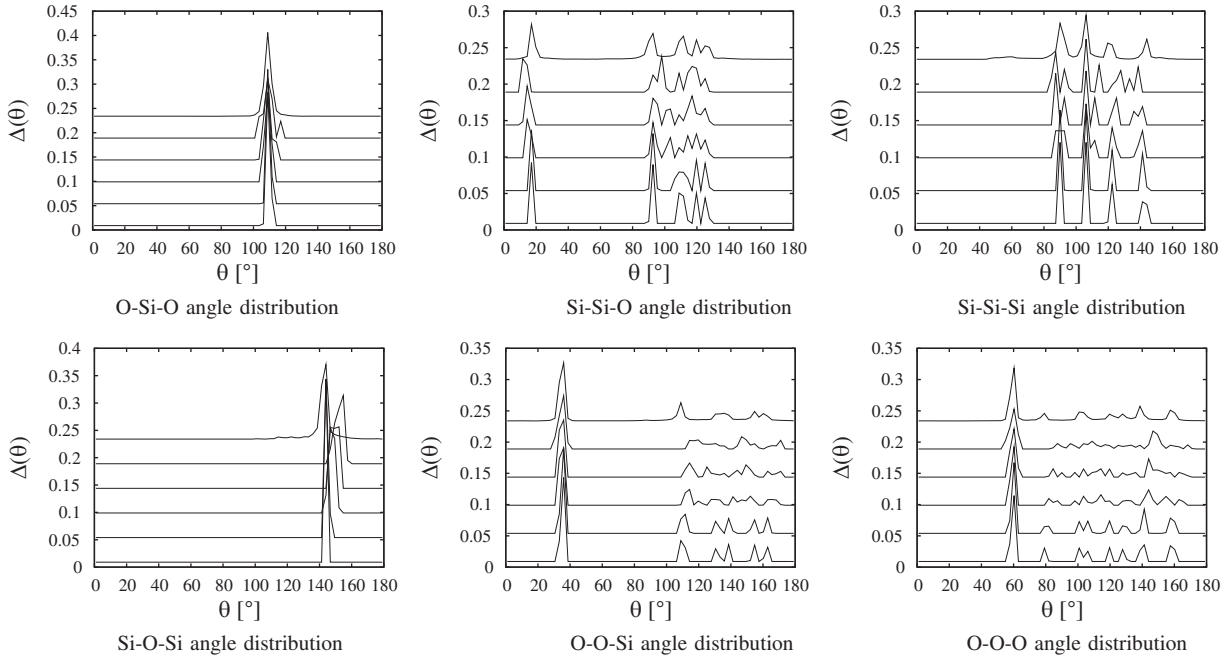

Fig. 3. We show the bond-angle distributions for the α-quartz−α-quartz-structures from runs at constant temperature. The lines in each figure correspond to different gap-sizes between the crystallites: 0, 0.4, 2.0, 2.8, 4.0 and 8.0 Å (bottom-up).

Si-tetrahedron. If the oxygens belong to different tetrahedrons the O–O–O angles are distributed from 80° to 160°.

Typically the broadening of peaks (especially of structural origin) is explained and caused by influences of the temperature. In Fig. 4 we show the temperature T calculated in sectors/layers (which have an equal size of 10% along the x-direction) vs. the position of the layers. On the left side of the figure the temperatures for structures of different (starting) gap-sizes are shown (0, 0.4, 2.0, 2.8, 4.0 and 8.0 Å from top to down). During the simulation no temperature gradients are applied. The temperatures are averaged over the last 20 ps and the standard deviations are calculated, respectively. If there is no gap present in the structure, a constant temperature can develop throughout the complete configuration (as can be seen in the uppermost plot on the left part of the figure). The initially introduced structures into the gap-sizes (separation of two sub-configurations up to 4 Å) can be closed and a constant temperature of 600 K is found in all layers of the structure. Typically, the standard deviation of the layers in the bulk, i.e. not the surface or the interface is about 5–10%. Only for the largest gap-size of 8 Å the barrier is not closed and a slightly larger standard deviation of the temperature at the boundary is observed. On the right side of the figure we show the temperature distribution of MD-simulations with temperature gradients (shown as dotted lines). For starting gap-sizes up to 4 Å in the structure the gradient can develop, since the gaps are closed and the energy can flow. If there are gaps between the two sub-configurations the temperature gradient cannot clearly develop since close to the gap the flow of energy is reduced and the temperature of the sectors close to the gaps deviates from the theoretical gradient line, i.e. close to the layer with low temperature the layers will have a reduced temperature and in the vicinity of the high-temperature layer the atoms develop higher kinetic energies. In case that the gap is not closed, the simulations using constant temperature are characterized by a change in the temperature deviation, and in the runs where we applied temperature gradients, a clear temperature jump of roughly 450 K is developed within a few Å instead of a continuous temperature gradient. This rather large deviation of the temperature of the surface layer is caused by the small number of atoms, since only less than 4% of the ensemble is comprising this sector and even this number fluctuates. This fluctuation is stable for even larger simulation periods (upto 5 ns).

3.2. ZSM-5–ZSM-5

For the ZSM-5 on ZSM-5-configurations comprising 1152 atoms we performed MD-runs at an averaged temperature of 600 K with an observation time of 100 ps and six different gap-sizes (0, 0.4, 2.0, 2.8, 4.0 and 8.0 Å). In a second modelling route we would like to estimate the influence of temperature gradients by fixing the temperature of two layers at temperatures of 300 and 900 K, respectively. In Fig. 5 we plot structures of ZSM-5 on ZSM-5. For the smallest gap with a width of 0.4 Å the surfaces coalesce, and a nearly perfect crystalline structure is built. In all other simulations with larger gap-size the surfaces do not coalesce. However, during the simulation partially disordered surfaces are developed where defects, e.g. new rings are formed.

From the total displacement one can derive the averaged atomic shifts, in the case of a starting gap with a width of 0.4 Å the atoms move 0.70 Å, and for the largest gap we find a displacement of 1.02 Å.

One should have in mind that different physical processes contribute to the motions. On one side there are thermal and vibrational motions which depend on temperature and do typically not exaggerate ca. 10% of the nearest-neighbour distance, on the other side there are contributions from relaxation and motions leading to the coalescence of the surfaces.

The results for the pair-correlation functions found in structures which are exposed to temperature gradients are very similar to the one described for the constant temperature simulations. Therefore, in Fig. 6 we show the pair-correlation functions $g(r)$ for the pairs Si–O, O–O and Si–Si, respectively, which stem from simulations performed at a constant temperature of about 600 K. In each figure the six different gap-sizes are shown from 0 Å (bottom) up to 8.0 Å (top). For the Si–O-distances we observe for all gap-sizes a strong and sharp first peak (nearest neighbour distance $r_{SiO}=1.65$ Å). In the

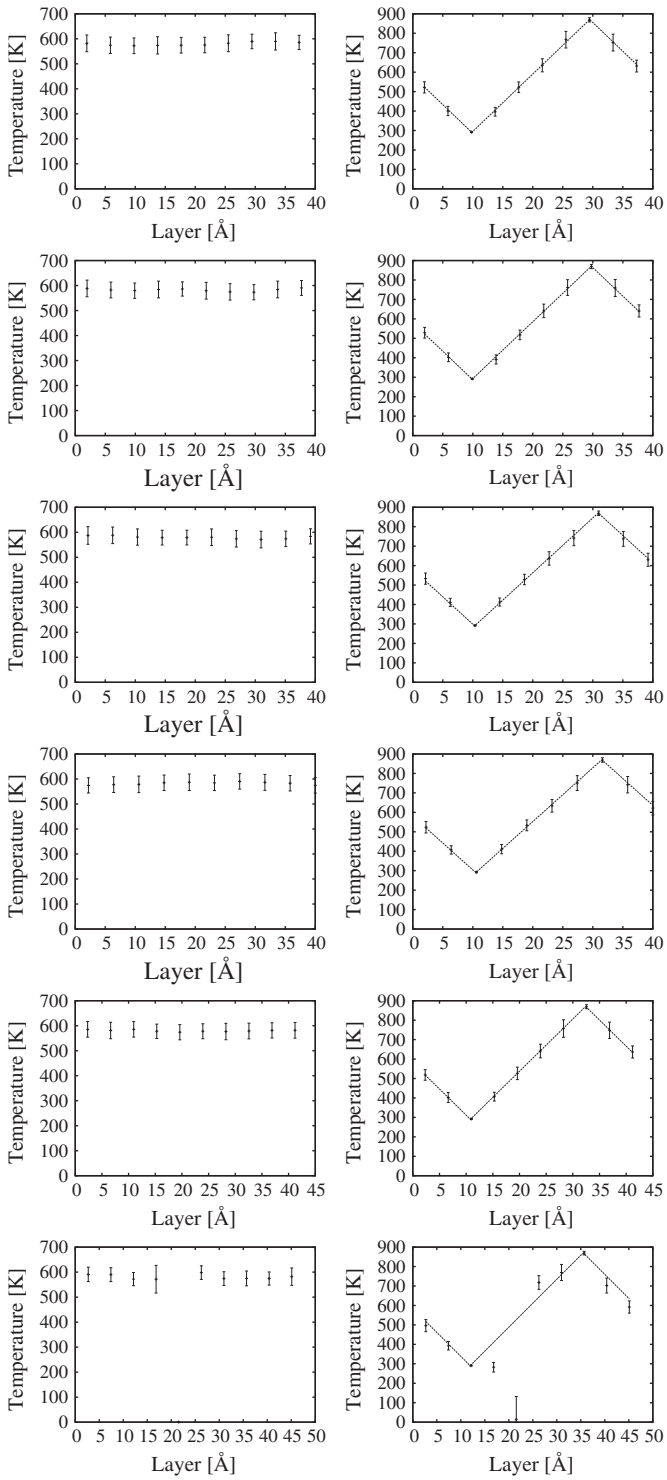

Fig. 4. The temperature distributions are displayed for the α-quartz−α-quartz-structures with different gaps between the crystallites (0, 0.4, 2.0, 2.8, 4.0 and 8.0 Å, from top to down). Left side: No temperature gradient is applied during the MD-simulations. Right side: During the simulations temperature gradients are applied, which are depicted by the dotted lines.

intermediate-range order a very slight broadening with increasing gap-size is observed. The peak at the first O–O-distance at 2.6 Å is quite sharp for all gap-sizes. This observation correlates with the narrow range of the tetrahedral angle (see Fig. 7). The intermediate-range order shows a very small broadening with increasing gap-size. For the Si–Si-distances the first peak at $r_{SiSi}=3.1$ Å a small shift (to lower distances) and a slight broadening can be seen, this finding is

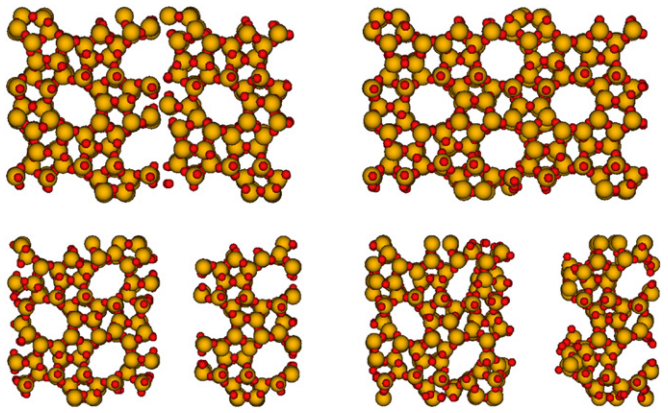

Fig. 5. Left: Starting configurations of the ZSM–ZSM-structures comprising 1152 atoms with gaps of 0.4 Å (top) and 8.0 Å (down) thickness. Yellow (light-grey) and red (dark-grey) spheres represent Si and O atoms, respectively. View is along the [0 1 0] direction. Right: Configurations after a constant temperature run with total displacement of $\Delta R \approx 24$ and 35 Å, respectively. (For interpretation of the references to colour in this figure legend, the reader is referred to the web version of this article.)

connected with the Si–O–Si angle distribution (see Fig. 7). At intermediate distances a clear shift and broadening of the peaks is observed.

The bond-angle distributions displayed in Fig. 7 result from constant temperature runs. As we have previously seen for the pair-correlation functions, the bond angles from different setups also exhibit similar distributions for all gap-sizes (from bottom to top the gap-sizes are 0, 0.4, 2.0, 2.8, 4.0 and 8.0 Å), i.e. no clear distinction can be made between the different modelling set-up, since the distributions of simulations with or without gradients cannot be discerned.

As we have seen from the α-quartz-α-quartz-structures the building unit is the SiO_4-tetrahedron which is only slightly distorted, since we measure a very sharp peak at 109° for the O–Si–O bond angle. The Si–O–Si distribution has the peak-position at 145° for all gap-sizes studied in our investigation, however with increasing gap-size the broadening of the peak becomes larger. Since this distribution is much broader compared to the one found in the quartz-structures, this gives a strong hint to the floppiness of the ZSM-network comprising flexible rings which surrounds pores and channels of different diameters. In the Si–Si–O angle distribution the peak at 15° stems from two silicons belonging to the same oxygen. This peak is directly connected to the Si-O-Si distribution, and similar to this rather broad distribution we observe a broad angle distribution. If the oxygen is not the bridging atom between the two silicons and is only neighbour to the ad-atom, the angle distributions range between 90° and 130° without any prominent features. The O–O–Si angle distribution shows a very prominent peak at 35° which is caused by oxygens belonging to the same tetrahedron, as we have seen for the quartz simulations. This result is in direct connection with the sharp tetrahedral peak in the O–Si–O angle distribution. This peak is stable for all gap-sizes which is -again- a strong hint for the stability of the tetrahedrons as building units. The peak distribution between 110° and 170° is much less pronounced compared to the results found in the α-quartz-structures, which points to a much less rigid network in the zeolite-configurations. For the Si–Si–Si angle distribution we find broad distribution of peaks between 90° and 150° which points to the different ring-sizes. With increasing gap-sizes the distribution will become smoother and even broader and reflect the additional ring-structures formed at the surfaces. The O–O–O angle distribution is governed by a strong peak at 60° (for all gap-sizes) which is caused by three

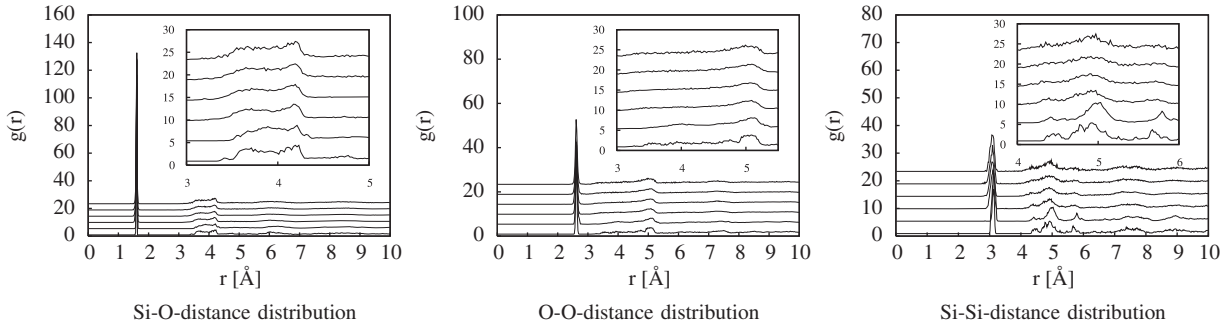

Fig. 6. The partial pair-correlation functions for the ZSM–ZSM-structures are shown. The lines in each figure correspond to different gap-sizes between the structures: 0, 0.4, 2.0, 2.8, 4.0 and 8.0 Å (bottom-up). The insets display the distance distributions for the intermediate regions. Results are presented from runs without temperature gradients.

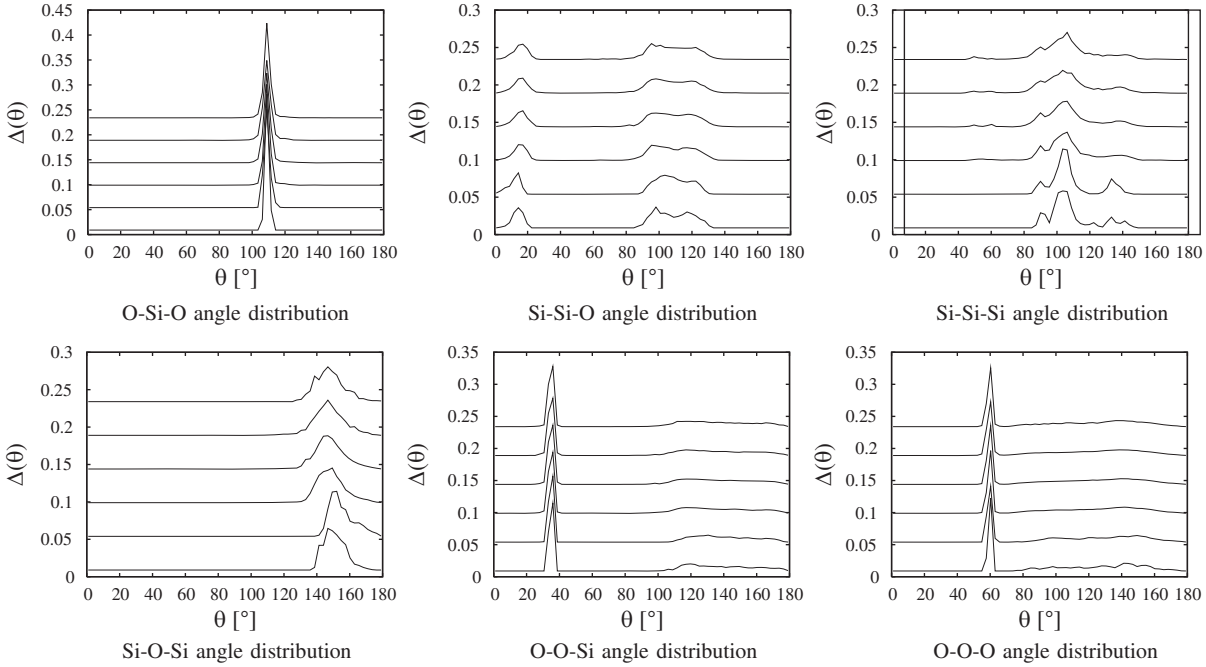

Fig. 7. We show the bond-angle distributions for the ZSM–ZSM-structures from runs at constant temperature. The lines in each figure correspond to different gap-sizes between the crystallites: 0, 0.4, 2.0, 2.8, 4.0 and 8.0 Å (bottom-up).

O which belong to the same Si-tetrahedron. If the oxygens belong to different tetrahedrons the O–O–O angles are broadly distributed from 80° up to 180°.

In Fig. 8 we show the temperature distribution in the ZSM-5 on ZSM-5-structures and plot the temperature T calculated in layers (the thickness of the layers is again 10% of the system-size) vs. the position of the layers. On the left side of the figure the temperatures for structures of different gap-sizes are shown (0, 0.4, 2.0, 2.8, 4.0 and 8.0 Å from top to bottom). During the simulations no temperature gradients are applied. The temperature of each layer is averaged over the last 20 ps and the standard deviations are calculated, respectively. If there is no gap or only a small gap (0.4 Å) present in the structure a constant temperature can develop throughout the complete configuration (as can be seen in the two uppermost plots on the left part of the figure). Splitting the structure into two parts and separating the two sub-configurations through gaps of distances 2.0, 2.8 and 4.0 Å leads to an increase of the temperature deviation (kinetic energy) at the border -up to three times larger than the average temperature deviation- with increasing gap-size. The increasing standard deviation of the temperature correlates the rather small number of atoms comprising the layers at the surface and since the atom number of the surface layer fluctuates all properties (e.g. velocities, temperature, density) changes, respectively. For the largest gap of 8 Å we observe that the range from 20 to 25 Å is filled with atoms only in the last part of the MD-simulation which leads to an—on average—smaller temperature.

On the right side of the Fig. 8 we show the temperature-distribution of MD-simulations with temperature gradients (shown as dotted lines). In the case that there is no gap or a very small gap in the structure the layers can develop a clear temperature gradient. If there are larger gaps between the two sub-configurations the temperature gradient cannot clearly develop since close to the gap the flow of energy is reduced and the temperature of the layers/sectors close to the gaps deviate from the theoretical gradient line, i.e. close to the layer with low temperature the layers will have a reduced temperature and in the vicinity of the high-temperature layer the atoms develop higher kinetic energies. The atoms at the boundary develop a rather high standard deviation of their kinetic energies which lead to a high temperature deviation at the gap.

In the case of the largest gap we observe for the simulation with temperature gradient that the gap is filled with a small number of atoms ($< 0.4\%$) at the end of the simulation which will lead to an extremely high standard deviation. However, the most important difference of the runs with temperature gradients compared with the constant temperature simulations is the

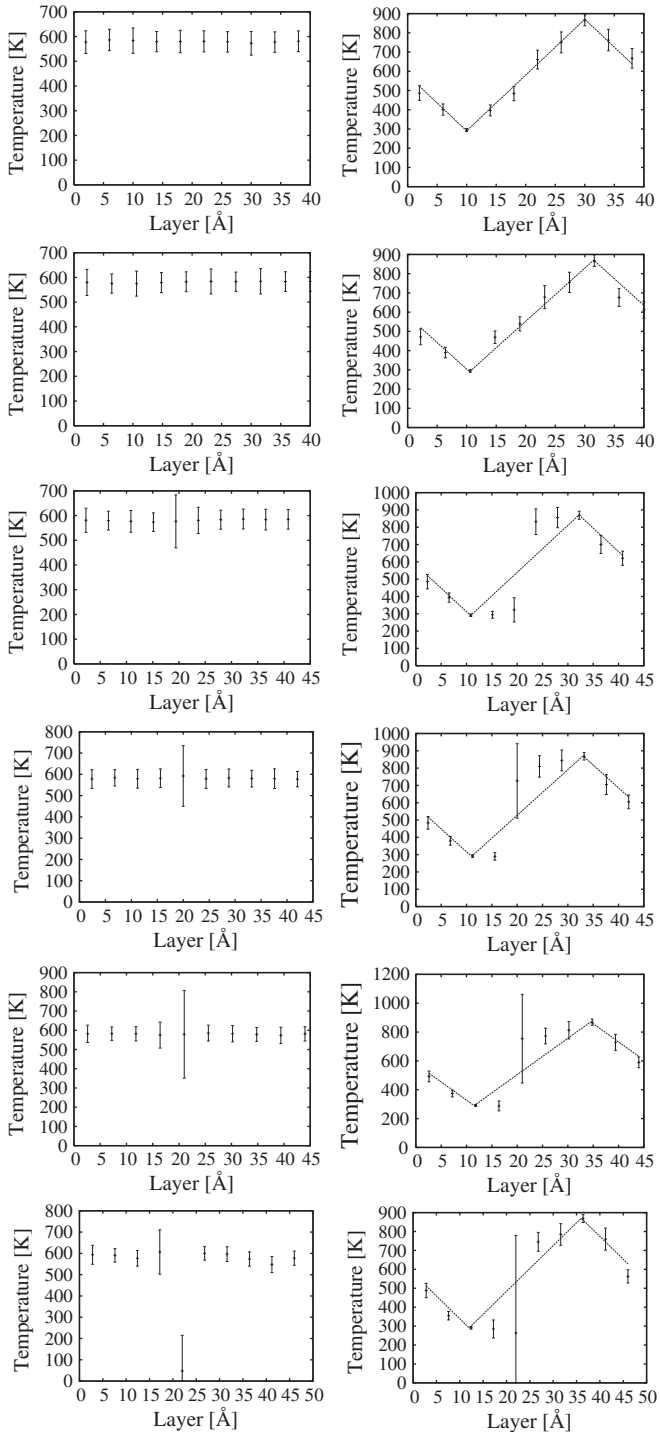

Fig. 8. The temperatures and their standard deviations are displayed for the layers of the ZSM–ZSM-structures with different gaps between the crystallites (0, 0.4, 2.0, 2.8, 4.0 and 8.0 Å) from top to bottom. Right: No temperature gradient is applied during the MD-simulations. Left: During the simulations temperature gradients are applied, which are depicted by the dotted lines.

development of a clear temperature jump of 500 K if surfaces are present in the structures. These deviations are stable for observation times of at least 2 ns.

3.3. α-Quartz−ZSM-5

We constructed two mixed configurations, a small system with 1296 atoms and a larger model comprising 4228 atoms. MD-simulations are again performed at $T=600$ K.

The small system is built using different spaces (0.5/1.0, 1.0/1.0, 5.0/1.0, and 10.0/1.0 Å) between the α-quartz- and ZSM-5-configurations which are aligned along the y-direction. In a second modelling route we would like to estimate the influence of temperature gradients by fixing the temperature of the layers at temperatures of 300 and 900 K, respectively. Two examples of the structures are depicted in Fig. 9. In the gap-sizes of up to 1.0 Å the surfaces coalesce to build interfaces which exhibit a rather disordered state. However, these structures are closed and the gaps vanish within the observation time. In the case of larger central gaps, the "inner" surfaces do not coalesce, however the smaller gap is closed caused by the coalescence of the surfaces due to periodic boundary conditions. The resulting interface and the remaining surfaces show a high degree of disorder or amorphization. The atomic displacements with values 2.15 and 1.82 Å, for gap-sizes 1.0/1.0 and 10.0/1.0 Å, respectively, reflect the fact that in the latter system only one gap (at the boundary) is closed whereas in the first model two gaps are closed.

In Fig. 10 we show the pair-correlation functions $g(r)$ for the pairs Si–O, O–O and Si–Si, respectively. The simulations were performed at a constant temperature of about 600 K. In each figure the four different gap-sizes are shown from 0.5 Å (bottom) up to 10.0 Å (top). For the Si–O-distances we observe for all gap-sizes a strong and sharp first peak (nearest neighbour distance $r_{SiO}=1.65$ Å). In the intermediate-range order no clear differences between the different gap-sizes can be discerned. The peak at the first O-O-distance at 2.6 Å is quite sharp for all gap-sizes. This observation correlates with the narrow range of the tetrahedral angle (see Fig. 11). The intermediate-range order seems to be independent of the gap-size. For the Si–Si-distances the first peak at $r_{SiSi}=3.1$ Å reveals a slight broadening with increasing gap-size, this finding is connected with the Si–O–Si angle distribution (see Fig. 11). Again there is no strong difference for the different gap-sizes at intermediate distances of the peaks.

No influence of the temperature gradient on the structure can be seen, i.e. the partial pair-correlation functions found in structures which are exposed to temperature gradients have the same patterns of distances compared to the constant temperature simulations.

The bond-angle distributions shown in Fig. 11 results from constant temperature runs. As we have previously seen for the pair-correlation functions the bond angles also show similar distributions for all gap-sizes (from bottom to top the gap-sizes are 0.5, 1.0, 5.0 and 10.0 Å). Similar to the partial pair-correlation functions the bond-angle distributions do not reveal differences from the different modelling set-ups, i.e. the distributions of

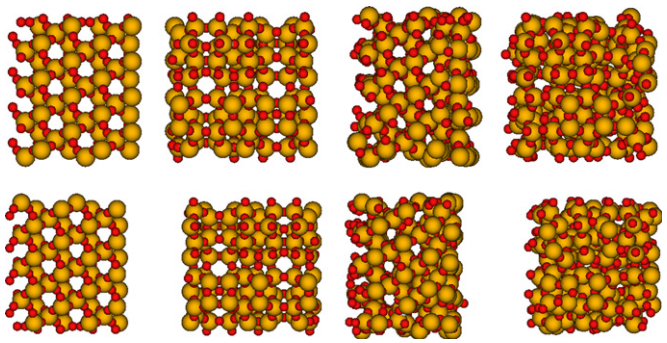

Fig. 9. Left: Starting configurations of the α-quartz−ZSM-5-structures comprising 1296 atoms with gaps of 1.0/1.0 Å (top) and 10.0/1.0 Å (down) thickness. Yellow (light-grey) and red (dark-grey) spheres represent Si and O atoms, respectively. View is along the [0 0 1] direction. Right panel: Configurations after a constant temperature run with respective total displacements of $\Delta R \approx 78$ and 65 Å. (For interpretation of the references to colour in this figure legend, the reader is referred to the web version of this article.)

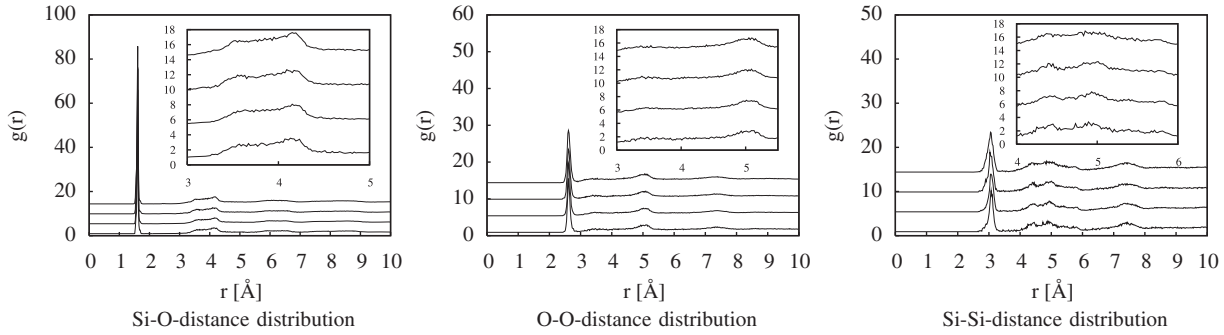

Fig. 10. The pair-correlation functions for the α-quartz−ZSM-structures are shown. The different lines in each figure correspond to different gap-sizes between the structures: 0.5/1.0, 1.0/1.0, 5.0/1.0, 10.0/1.0 Å (bottom-up). The insets show the intermediate regions. Results are presented from runs without temperature gradients.

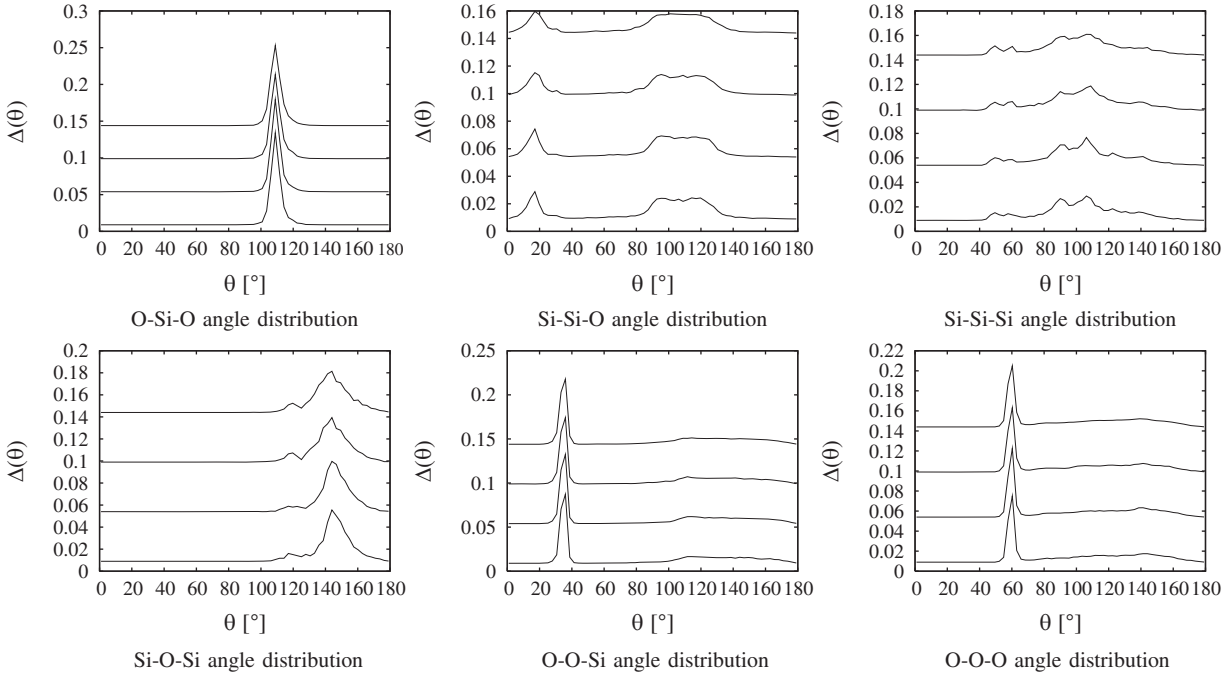

Fig. 11. We show the bond-angle distributions for the α-quartz−ZSM-structures from runs without temperature gradients. The different lines in each figure correspond to different gap-sizes between the crystallites: 0.5/1.0, 1.0/1.0, 5.0/1.0, 10.0/1.0 Å (bottom-up).

simulations with or without gradients cannot be discerned. As we have seen from the simulations comprising quartz- or ZSM-5-crystallites the building unit is the SiO_4-tetrahedron which is not distorted, since we measure a very sharp peak at 109° for the O–Si–O bond angle. For increasing gap-size a slight broadening can be seen. The Si–O–Si distribution has a peak at 145° with a shoulder at 120° for all gap-sizes studied in our investigation. However, with increasing gap-size a small broadening of the (main) peak occurs. Since this distribution is much broader compared to the one found in the quartz-structures and even broader than those found in the ZSM-5-configuration, this gives a strong hint to the floppiness of the mixed network. In the Si–Si–O angle distribution the peak at 15° stems from two silicons belonging to the same oxygen. This peak is directly connected to the Si–O–Si distribution, and similar to this rather broad distribution we observe a broad angle distribution. If the oxygen is not the bridging atom between the two silicons and is only neighbour to the ad atom the angle distributions ranges—without any striking features—between 90° and 130°. The O–O–Si angle distribution shows a very prominent peak at 35° which is caused by oxygens belonging to the same tetrahedron, as we have seen for the quartz simulations this result is in direct connection to the sharp tetrahedral peak in the O–Si–O angle distribution. This peak is stable for all gap-sizes which is—again—a strong hint for the stability of the tetrahedrons as building units. The peak distribution between 110° and 170° is—similar to the ZSM-network—much less pronounced compared to the results found in the SiO_2-structures, which points to a much less rigid network. For the Si–Si–Si angle distribution we find a broad distribution of peaks between 50° and 180° which do not depend on the gap-sizes. The O–O–O angle distribution is governed by a strong peak at 60° (for all gap-sizes) which is caused by three O which belong to the same tetrahedron. If the oxygens belong to different tetrahedrons the O–O–O angles are broadly distributed from 80° to 180°.

The temperature distributions are shown in Fig. 12. The resulting temperature distribution of runs with constant temperatures are plotted at the left panel of the figure. In the structures with the smallest gaps the temperature can develop throughout the system. The temperature distribution is interrupted in those configurations which have a gap-size larger than 5 Å, for the largest gap 10 Å we observe a rather large temperature deviation in the layer close to the gap, due to the fact that less than 0.4% of the atoms are present in the surface layer. In this respect it is interesting to mention that the small gap of 1.0 Å—at

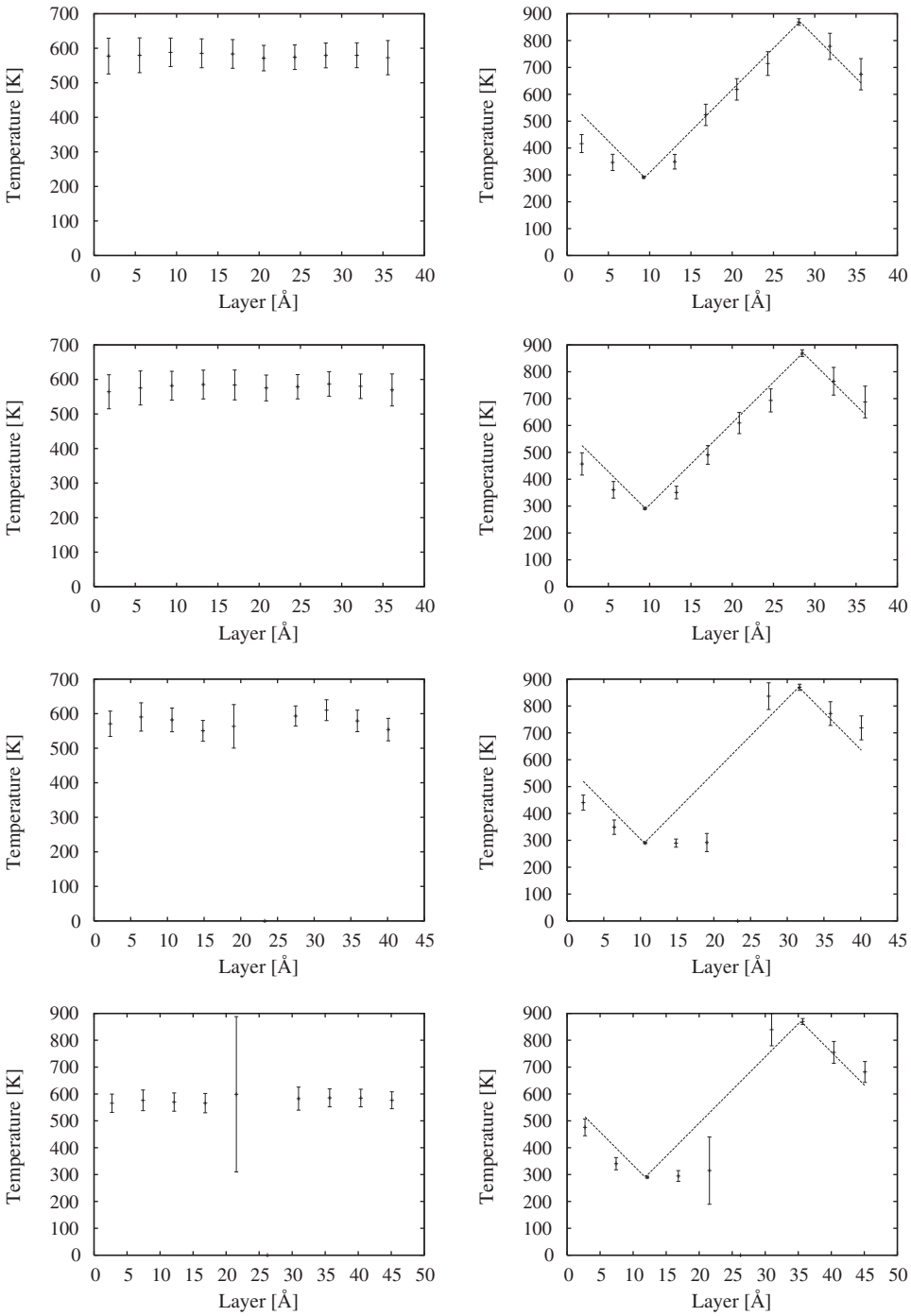

Fig. 12. The temperatures and their standard deviations are displayed for the layers of the α-SiO_2−ZSM-structures with different gaps between the crystallites (0.5/1.0, 1.0/1.0, 5.0/1.0, 10.0/1.0 Å from top to bottom). Left side: No temperature gradient is applied during the MD-simulations. Right side: During the simulations temperature gradients are applied, which are depicted by the dotted lines.

the left boundary of the structures is closed within all simulations. Using temperature gradients in the simulation we observe that the smallest gaps are closed during the simulation since clearly temperature gradients can develop in the structures. For the larger gap-size the energy distribution is hindered and at the layers close to the gaps a temperature difference is established and as seen in the constant temperature runs the layer close to the gap exhibit a larger temperature deviation compared to the rest of the system. Since the small gap of 1.0 Å is closed during the simulation a gradient can develop in that part of the structures.

The second mixed system comprising an α-quartz with 2520 atoms and a ZSM-5-crystallites of 1728 atoms aligned in *x*-direction with gap-sizes 0.1/0.2, 0.5/1.0, 1.0/2.0, 1.5/3.0, 2.0/4.0 and 4.0/8.0 Å. We performed both constant temperatures runs at 600 K and applied temperature gradients. Two examples of the starting structures are shown in the left panel of Fig. 13 whereas the tempered configurations are given at the right side of the figure. In all cases, the inner lying surfaces coalesce to form a partially disordered interface. The gaps (due to periodic boundary conditions) are only closed for a width less than 1 Å. Therefore, the

additional interface in the model (shown on top of the figure) generates further disordered parts in this configuration. In all other cases, the remaining surfaces (caused by the boundary conditions) have a less degree of amorphicity compared to the interface in the centre of the models. From the total displacements one calculates the atomic shifts from 1.27 up to 2.64 Å, which increase linearly with the gap-sizes (0.5/1.0 up to 4.0/8.0 Å, respectively).

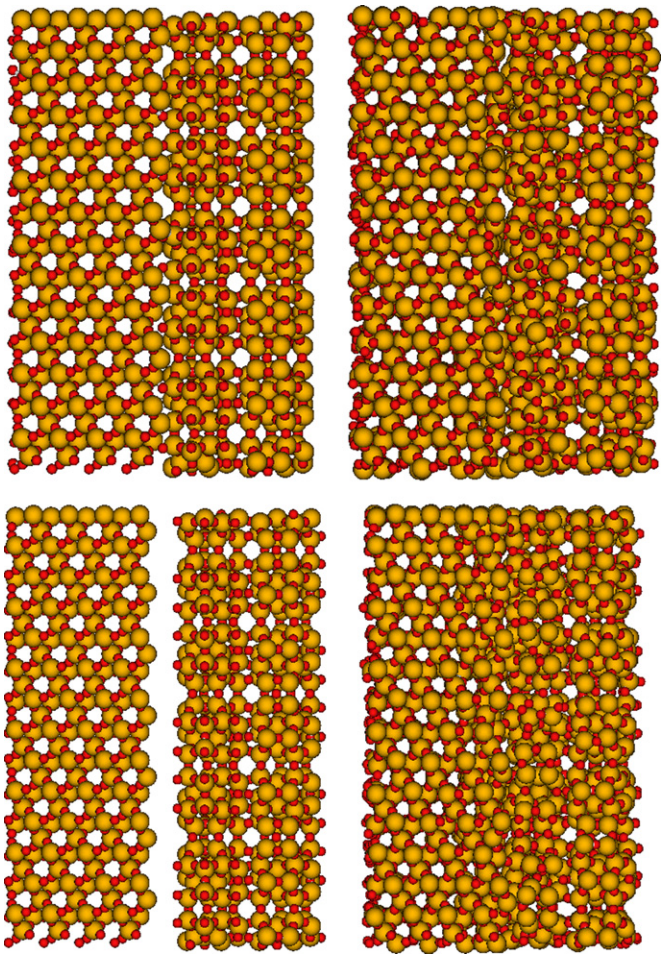

Fig. 13. Left: Starting configurations of the α-quartz−ZSM-structures comprising 4248 atoms with gaps of 0.5/1.0 Å (top) and 4.0/8.0 Å (down) thickness. Yellow (light-grey) and red (dark-grey) spheres represent Si and O atoms, respectively. View is along the [0 0 1] direction. Right panel: Configurations after a constant temperature run with respective total displacements of $\Delta R \approx 83$ and 172 Å. (For interpretation of the references to colour in this figure legend, the reader is referred to the web version of this article.)

In Fig. 14 we show the pair-correlation functions $g(r)$ for the pairs Si–O, O–O and Si–Si, respectively. The simulations were performed at a constant temperature of about 600 K. In each figure the six different combinations of gap-sizes are shown from the smallest (bottom) up to the largest one (top). For the Si–O-distances we observe for all gap-sizes a strong and sharp first peak (nearest neighbour distance $r_{SiO}=1.65$ Å). In the intermediate-range order (shown in the inset) one can observe that for the larger gap-sizes more structural features in the distance pattern can be seen compared to the small distances. The peak at the first O–O distance at 2.6 Å is quite sharp for all gap-sizes. This observation is in agreement with the narrow range of the O–Si–O bond angle (see Fig. 15). Around 5 Å (see inset) a double peak is found for larger gap-sizes whereas for small gaps a broad distribution is found. Also for the first peak of the Si–Si-distances at $r_{SiSi}=3.1$ Å we cannot recognize any broadening of the peak for the different gap-sizes, this finding is correlated with the Si–O–Si bond-angle distribution (compare with Fig. 15). Looking at the inset one clearly observes more structural features with increasing gap-sizes.

The results for the pair-correlation functions found in structures which are exposed to temperature gradients are comparable to the constant temperature simulations, i.e. we find the same patterns of distances. Especially the—at a first glance—astonishing observation of clear patterns with increasing gap-sizes is confirmed which may give a hint to the reduced amorphicity of the surfaces at the boundaries which do not coalesce to form a potentially disordered interface. In contrast to the first mixed model the partial pair correlation of the Si–Si distance distribution has more features in common with the distribution of α-quartz, whereas in the Si–O- and the O–O-distributions not all details of the α-quartz-distributions are reproduced. However, the partial pair-correlation functions exhibit more peaks similar to quartz than the respective distributions in ZSM-5. Therefore, in this type of mixed configuration the ZSM-structure seems to be more affected by disorder than the α-quartz-part of the system.

The bond-angle distributions displayed in Fig. 15 resulted from constant temperature runs, from bottom to top the different gap-sizes are 0.1/0.2, 0.5/1.0, 1.0/2.0, 1.5/3.0, 2.0/4.0 and 4.0/8.0 Å.

As already seen in the partial pair-correlation functions no clear distinction can be made between the different modelling set-ups, i.e. the bond-angle distributions of simulations with temperature gradients are similar to those presented above. The building unit—based on only slightly distorted SiO_4-tetrahedrons—is again confirmed since we measure a very sharp peak at 109° for the O–Si–O bond angle, a dependence from the gap-size cannot be figured out. The Si–O–Si distribution has a peak-position at 145° with a slight shoulder at 120° for all gap-sizes studied in our investigation, with increasing gap-size a small sharpening of the (main) peak occurs. The distribution is broader

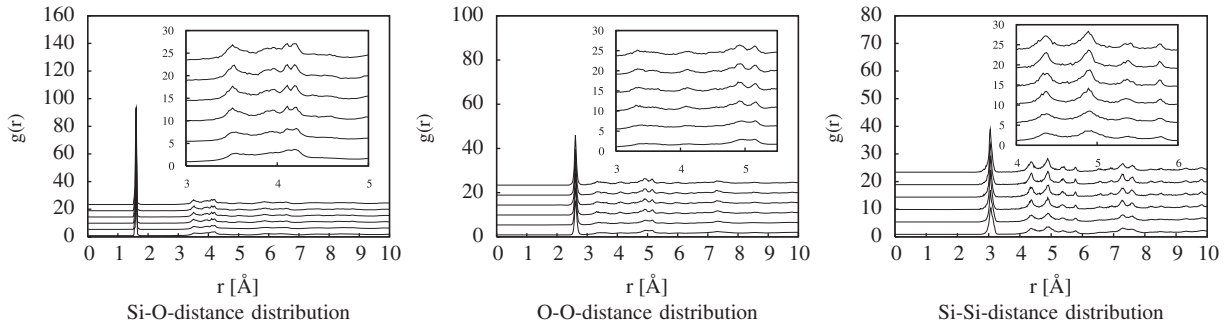

Fig. 14. The partial pair-correlation functions for the α-quartz−ZSM-structures are shown. The different lines in each figure correspond to different gap-sizes between the structures: 0.1/0.2, 0.5/1.0, 1.0/2.0, 1.5/3.0, 2.0/4.0 and 4.0/8.0 Å (bottom-up). The insets show the distance distributions for the intermediate regions. Results are presented from runs without temperature gradients.

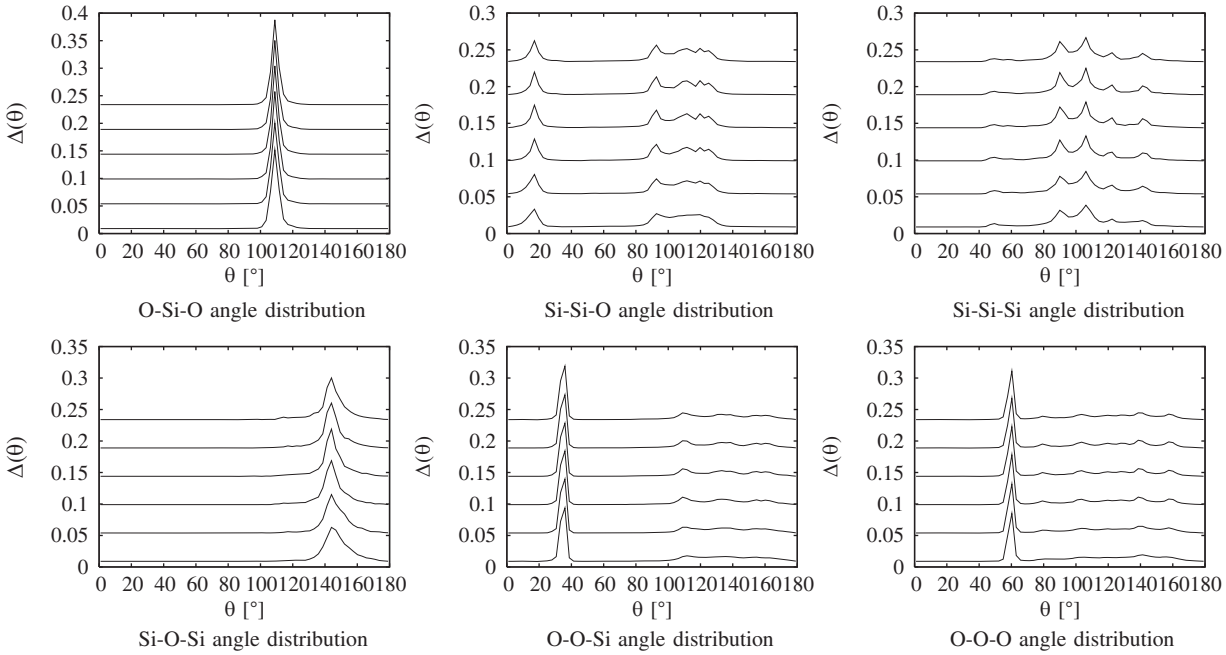

Fig. 15. We show the bond-angle distributions for the α-quartz−ZSM-structures from runs without temperature gradients. The different lines in each figure correspond to different gap-sizes between the crystallites: 0.1/0.2, 0.5/1.0, 1.0/2.0, 1.5/3.0, 2.0/4.0 and 4.0/8.0 Å (bottom-up).

compared to the one found in the quartz-structures, however the distribution is comparable to those found in the ZSM-5-configuration. In the Si–Si–O angle distribution the peak at 15° stems from two silicons belonging to the same oxygen. In the case that the oxygen is not the bridging atom between the two silicons and is only neighbour to the ad-atom the angle distributions ranges between 90° and 130°, with increasing gap-size a clear peak-structure develops. The O–O–Si angle distribution shows a very prominent peak at 35° which is caused by oxygens belonging to the same tetrahedron, from a geometric point of view this result is directly connected to the sharp tetrahedron peak in the O–Si–O angle distribution. This peak is stable for all gap-sizes which is—again—a strong hint for the stability of the tetrahedrons as building units. The peak distribution between 110° and 170° is comparable to the results found in the ZSM-structures and gives hints to the flexibility of the network. For the Si–Si–Si angle distribution we find a broad distribution ranging from 50° up to 160° with two small peaks at 90° and 110° which do not depend on the gap-sizes. The O–O–O angle distribution is governed by a prominent peak at 60° (for all gap-sizes) stemming from the three O-atoms at the same Si-tetrahedron. If the oxygens belong to different tetrahedron the O–O–O angles are broadly distributed between 80° and 180°.

The results of the temperature distributions are shown in Fig. 16. In this type of structure we implemented two different gap-sizes, the smaller gap is placed in the centre of the structure whereas the larger gap is situated at the boundary of the system. The temperature distribution from the runs using constant temperatures are plotted at the left panel of the figure. During all simulations the smaller gap—in the centre of the structure—is closed within the simulation period. Consecutively a constant temperature can develop through the ''inner'' part of the structure. Only for the two smallest gap-sizes at the boundary the energy can flow and a constant temperature is established throughout the complete structure. If the gaps at the boundary are larger than 2 Å one observes that the layer close to the boundary has a larger temperature deviation than the others, i.e. despite periodic boundary conditions the surfaces do not coalesce and cannot close the gap. Application of temperature gradients in the simulation yield similar results, again we find the (smaller) gap in the centre to be closed within the observation time which means that in the inner part of the system a temperature gradient has developed (for all gap-sizes). For a gap-size at the boundary which is smaller or equal to 1 Å the energy can flow via periodic boundary conditions and a temperature gradient is established in the complete system. However, if the boundary gap is larger than 2 Å the energy distribution is hindered and at the layers close to the gap a temperature difference is established and as seen in the constant temperature runs the layer close to the gap exhibit a larger temperature deviation compared to the rest of the system. The rather large temperature deviations are (again) correlated to the corresponding small and fluctuating numbers of atoms at the sector close to the surface at which only $< 1\%$ of the total ensemble are present.

4. Discussion

The focus of our simulation is mainly laid on structural and thermal properties of crystalline quartz-systems, zeolite-structures and combinations of them. The interpretation of our results is purely qualitative, since quantitative or experimental results, especially for the temperature distributions are not (yet) available.

A first striking result of simulating one species of crystals is that small gaps will be closed and nearly perfect crystalline boundaries are generated instead of these gaps. In the simulations of different combinations of systems, small gaps are also closed, however disordered interfaces are generated, since the crystalline units are too different to match perfectly. This observation is independent from the different computational set-ups which we applied, i.e. whether we use a constant temperature simulation or apply temperature gradients, the results are similar. Introducing larger gaps reveal fundamental differences between the α-quartz-structures and the one based on ZSM-5-configurations. The tendency to overcome gaps is more pronounced in α-quartz compared

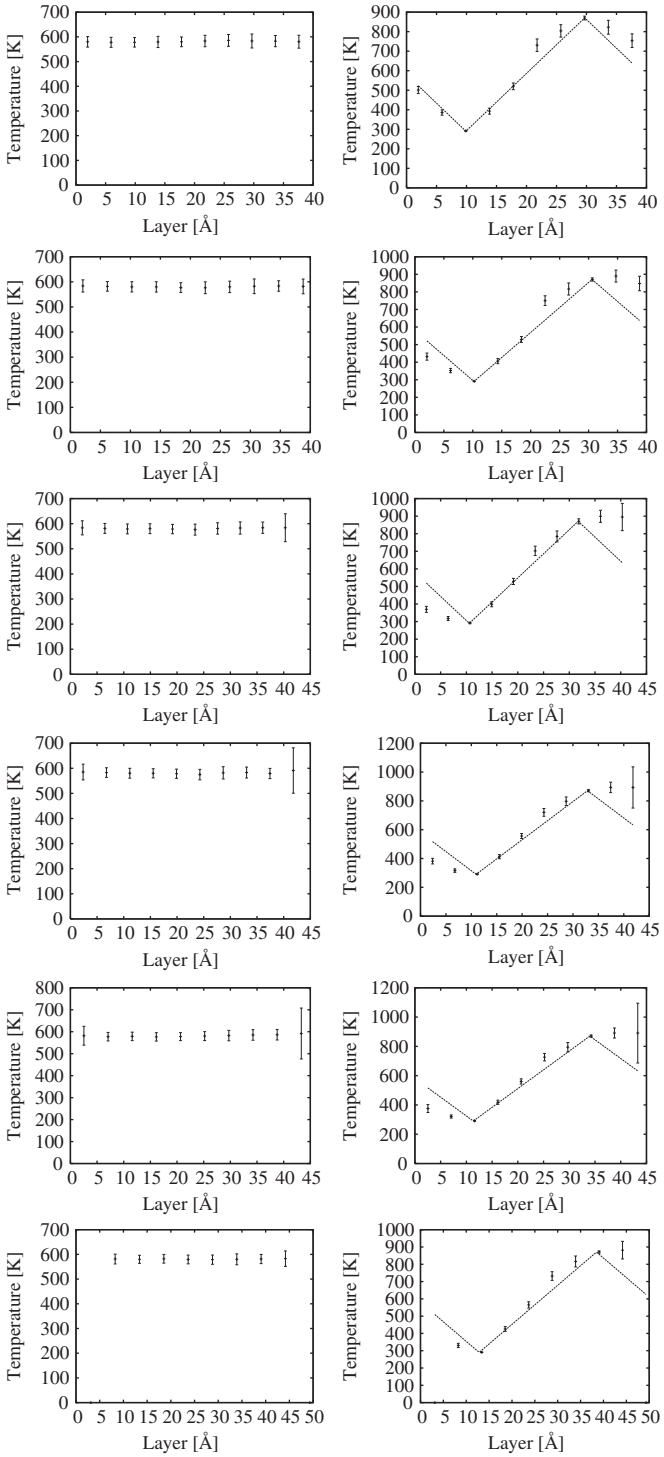

Fig. 16. The temperatures and their standard deviations are displayed for the layers of the α-quartz−ZSM-structures with different gaps between the crystallites (0.1/0.2, 0.5/1.0, 1.0/2.0, 1.5/3.0, 2.0/4.0 and 4.0/8.0 Å from top to bottom). Left side: No temperature gradient is applied during the MD-simulations. Right side: During the simulations temperature gradients are applied, which are depicted by the dotted lines.

to ZSM-5, since a gap of 4 Å is closed by the quartz-structure whereas the ZSM-5-system can only overcome gaps less than 2 Å.

Having a closer look at the different configurations reveal the influence of structural properties on dynamic behaviour and thermal/temperature development. First we would like to focus on the dynamic processes in the structures which lead to the coalescence of the surfaces at the introduced small gaps. Despite the fact that the two main systems are based on SiO_4-tetrahedrons the crystalline arrangements lead to differences in the densities, i.e. the density of α-quartz is $\rho = 2.63\ g/cm^3$ and the density of ZSM-5-zeolite is $\rho = 1.78\ g/cm^3$. Let us first consider the system with the highest density, i.e. the configurations built by α-quartz-structures. For these structures we have introduced a gap in the centre of the configuration, the sizes of the gaps are: 0, 0.4, 2.0, 2.8, 4.0 and 8.0 Å. Since we applied constant volume simulations the α-quartz-configurations closing a gap up to 4 Å reduce their density. The coalescence of the surfaces at gaps with distances up to 4 Å is possible because the atoms near the gap have enough "binding" sites. However, in order to close the gaps of this size, it is necessary to slightly distort the building unit and its crystalline arrangement. Of all simulated systems the pure α-quartz-structures show the smallest atomic displacements which hints to a small degree of disorder or to a small number of defects introduced into these structures. The effects of a strongly conserved crystallinity are also reflected in the partial pair-correlations and bond-angle distributions. So, the observed shifts in the distances (see the slight shifts of the O–O- and Si–Si-distances shown in Fig. 2) caused by the increase of the O–Si–O bond angle and especially of the Si–O–Si bond angle (see Fig. 3) can explain the stretching of the tetrahedrons which is necessary to overcome the gaps and to cause the coalescence of the surfaces. Since the nearest-neighbour distance Si–O is not affected throughout the simulations at least at the moderate temperature which we considered, a crucial role is played by the bond angles in the quartz-structure. A further increasing of the Si–O–Si bond angle up to 180° without stretching of the Si–O-bond-distance, i.e. the structure would be transformed in analogy to the α- to β-cristobalite transition [66], could overcome a gap of 4.8 Å for the considered system size. However, one should also keep in mind that not only structural features but also the interatomic potential between the atoms are responsible for an attractive behaviour. So at a distance of 8 Å—the largest gap we simulate—the interactions between a Si- and an O-atom are governed by the Coulomb-interaction which is reduced to ca. 20% in comparison of the nearest neighbour energy. Therefore, for a quartz-structure with a gap larger than 8 Å it may be energetically favoured to create new bonds at the central surfaces, even if this may introduce some surface defects, instead of closing the gap.

The second type of system which we studied has a much smaller density. A perfect ZSM-5-structure has a density of only $1.78\ g/cm^3$. Introducing gaps reduces the average density from 1.70 to $1.48\ g/cm^3$. The smaller the density of a system is the smaller is the possibility of an atom to have interaction partners within a typical range. This may explain the fact that in the zeolite-system a gap of 2.8 Å is already sufficient to leave the system split. In a much denser system like the α-quartz the atoms have enough possible binding sites at least within a range of 4 Å to close a gap of respective size. The relatively large averaged atomic displacements (up to 1.32 Å per atom) point to an accordingly large flexibility of the ring-structures or to large structural rearrangements of entities beyond single tetrahedrons, which are not too much affected in the simulations. Since the gaps are only closed in case of the smallest one, these atomic shifts also reflect the degree of disorder and amorphicity introduced into the structures. This observation is also supported by previous simulations of structural properties of zeolite-based systems from which we learned that the flexibility of the structure is caused by the variability to generate ring-structures [61]. Having this in mind, one can argue that it is energetically favourable for the atoms to form small rings together with the neighbouring atoms and thereby reducing the number of dangling

bonds at the surface (see Fig. 5) instead of considerably reducing the gap by a coalescence of opposite surfaces. Therefore, both the broadness of the Si–O–Si bond angle and the, thus consequently caused, change of the Si–Si-distances (see Fig. 6) reflect the floppiness of the network and give a strong hint towards the different ring sizes, which are generated, in order to saturate the dangling bonds at the surface. However, this behaviour leads to an increase of the structural surface defects by the formation of new rings, which differ from the "bulk" rings. A rough and qualitative estimate of the degree of disorder or number of defects at the surfaces close to the gap may be seen from the standard deviation of the temperature in the respective layers. For the ZSM-5-configurations we measure with increasing gap-size an increasing standard deviation of the temperature at the position of the surfaces. Compared to the α-quartz-structures this effect is much larger and sustain the impressions which one gets from the structure (compare Figs. 1 and 5). Therefore, the probability to have defects or disorder at the surface is larger in the ZSM-5-configuration than in the α-quartz-structure.

In the mixed systems, which necessarily will have two gaps, we investigated two different situations: in the first combination, which comprises 720 atoms of an α-quartz-structure and 576 atoms in a ZSM-5-configuration aligned in *y*-direction, one gap—at the boundary—has a size of 1.0 Å, whereas for the second gap in the centre we have chosen sizes ranging from 0.5 up to 10 Å. The gap at the boundary (with a size of 1.0 Å) is closed in all simulations. However, the gap in the centre will not be closed for distances larger than 5 Å. Again one can argue, that—due to the interaction range of the potential—the attractions between atoms lying on opposite sites of the gap are too small to lead to a coalescence of the surfaces. What makes the situation even more complicated is the fact, that—in contrast to the previous simulations—the sub-systems do not match and therefore, only disordered interfaces are generated or surface defects are developed at the borders close to the gap. As we have previously seen the partial amorphization of the system is a favoured strategy in order to reduce the surface defects, which are caused by the dangling bonds of the generated interface at the beginning of the simulation. This amorphization can also be deduced from the relatively large values found in the atomic shifts which range from 1.69 up to 2.15 Å per atom. Here one should have in mind that these shifts contribute partially to the coalescence of surfaces and therefore, a large part is due to local changes of the structures.

What is really striking is the fact that the partial pair-correlation functions of this mixed system have a higher similarity to the peak-distributions of the ZSM-5-systems than to the α-quartz-structures, this can be interpreted that the ZSM-5-system is relatively more conserved and that vice versa the α-quartz-structure is more disturbed.

To check whether system size or orientation of the structures play a crucial role we investigated a second model. In the second mixed model we aligned an α-quartz of 2520 atoms in *x*-direction with a ZSM-5-structure of 1728 atoms. Since the sub-structure do not match, the complete structures have two gaps. One gap is established in the centre where the two structures are combined, and a second gap is generated at the boundary where periodic boundary conditions are applied. The construction is designed such that the central gap is always half as large as the boundary's gap. The central gap, which is smaller than 4 Å in our study, is closed in all considered models. This explains the very large averaged atomic shifts up to 2.64 Å, which linearly increase with the gap-sizes, i.e. a fraction of the atomic displacements contributes to the coalescence of the surfaces. Nevertheless, the largest part of the shifts is due to introduce defects or disorder into the configuration.

The gap at the boundary is only closed for those cases in which the distance between the opposite sites is smaller than 3 Å. The generated interfaces show a disordered structure compared to the those parts of the systems which are far apart from the "inter-structural" borders. From the structures (see Fig. 13) one can inspect that the ZSM-5-part of the configuration is more affected by the amorphization of the interface compared to the α-quartz-configuration. This observation may be understood from the floppiness of the ZSM-5-network which is also expressed in the broadness of the Si–O–Si bond-angle distribution with a broad peak at an angle of 140–145° and a (small) shoulder at 120°. The main difference of the two mixed systems is the alignment of the sub-structures and the construction of the gaps introduced in the configurations. The difference in the system sizes plays a minor role, since the larger system is generated by the elongation of the structure in only one direction ($b=59.70$ Å). Both, the dimension *c* (27 Å) and the size along the direction of the alignment (40–50 Å) are similar in both mixed structures. Comparing the structural models the smaller system is much more disordered than the larger structure. With increasing gap-size both the interface (due to periodic boundary conditions) and the surfaces (in the centre of the structure) show an increase of the degree of amorphization. Whereas the larger system shows (partial) disordered interfaces (in the centre) and even less disordered surfaces (due to periodic boundary conditions) which have a decreasing number of surface defects with increasing gap-size.

However, not only structural properties like bond angles give hints to the degree of amorphization, it can be also deduced from the temperature evolution in the vicinity of the surface. The kinetic energy of the atoms forming surface defects show a larger deviation than the atoms of more crystalline parts in the structure.

Thermal properties are often important for the materials' functionality. Therefore, we focus in our further discussion on the temperature development and on thermal properties. A general observation is related to the temperature development in the structures and the equipartition theorem. In those structures which have no gaps or in which the gaps are closed by coalescence of the surfaces within the observation time, it does not matter whether the interface is amorphous, has defects or is crystalline, the temperature is equally distributed throughout the configuration and the heat can flow without any borders or distortions. Therefore, the temperature in the structure without application of a temperature gradient is really constant and the temperature standard deviations in the different layers are equal. Changing the experimental set-up such that one layer is cooled to a low and another layer is heated to a high temperature, leads to the development of a temperature gradient in the structures which have no gaps or where the gaps are closed, i.e. the heat can flow, since there are no borders and a gradient can clearly develop. Astonishingly, the number of defects or the degree of amorphization is irrelevant for the development of a temperature gradient and even the standard deviation of the temperatures is not influenced by structural details.

In those models where initially the structures generated surfaces remained throughout the MD-simulations, these act as heat barriers in qualitative agreement with experiments [1,9,10]. The keyword here is heat resistivity, i.e. the energy flow or the heat transport through this part of the configuration is at least considerably reduced or even completely vanished. However, not only the presence of surfaces reduces the heat flow, the gap itself will also play an important role. This is caused by the range of atomic interactions, which is reduced with increasing distance. Therefore, in the case of constant temperature runs one can clearly see that, for those structures where a gap is present between the two sub-structures throughout the observation time,

there is an additional (to the heat resistive) barrier at the surfaces. Compared to the layers of the bulk and depending on the gap-size and the type of system a larger standard deviation of the temperature is observed at the surfaces, which hints especially to an increase of the number of defects or the degree of disorder at the barrier. Change of the computational set-up from constant temperature to the application of a temperature gradient, i.e. heating one layer to a high temperature and cooling a second layer to a low temperature will not lead to a (continuous) temperature gradient in the structure since at the surfaces a temperature jump (a little less than the applied temperature difference) is established. For those runs where we applied temperature gradients the energy transport is stopped or at least hindered and a temperature difference at the boundary occurs. These findings can be explained by the mismatch or the interruption of the phonons in such "broken" systems [1], i.e. the energy cannot be exchanged between the surfaces (remember the simulation is *in vacuo*) therefore, the heated layer causes a hot surface whereas the cooled layer generates a cool surface.

5. Summary and conclusion

Typically molecular dynamics simulations are used to investigate bulk effects. Here we study the influence of surfaces or interfaces on structural and thermal properties. Introducing different gap-sizes in crystalline configurations is useful to investigate surfaces between structures or the development of boundaries/interfaces. The gaps, which we introduce at the beginning of the simulation into the starting configurations, split the systems into two sub-structures and range up to 10 Å.

In the case of the α-quartz−α-quartz we observe a coalescence of the two surfaces up to a distance of 4 Å. For the quartz-based structures which are investigated we observe that the nearest neighbour distance Si–O is not affected by the simulation and has no influence on these arrangements, most important for the collective motions are the changes of the bond angles. The observed coalescence leads to a (nearly) perfect crystalline interface. In order to establish a crystalline interface, it is necessary to have delocalized modes of the atoms which match in two similar crystallites. This extended motion is mainly due to an enlargement of the Si–O–Si bond angle with increasing starting gap-size. In the case of zeolite-based ZSM-5–ZSM-5-structures only the smallest gap is closed by structural rearrangements. The surfaces are introduced by cutting rings of different sizes (five-membered, six-membered and ten-membered rings are affected) and thus ring-deformations and strongly distorted rings are generated. Therefore, one can easily imagine, that the nearest neighbour distance of the silicon and oxygen atoms, which is too stable to significantly contribute to an extension of the structure, could not lead to a coalescence of the surfaces. Also, one should have in mind that the relatively small density of the system is not sufficient to have enough interaction partners on both sides of the gap which could sustain a coalescence over a distance comparable to a typical nearest-neighbor distance. However, since sub-systems are of equal type, the coalescence of (very) close surfaces generates a perfectly crystalline interface. In order to undo the deformation or the tilt of the rings caused by a small gap, a much more complicated motion is necessary, since also an ordinary change of bond angles—as it is the case for α-quartz—would not be sufficient to explain the twists and rotations of the rings or ring-fractures. To identify the motions of the coalescing surfaces a mode-analysis [14,20,60,67] would be helpful, but this was not the focus of the work presented here. In contrast to the systems comprising only one type of species, structures including different sub-systems develop (partially) disordered interfaces, because from a structural point of view the opposite atoms do not match and from a dynamical point of view the modes are broken at the surfaces (for the trapping/stopping of phonons, see discussions in Refs. [1,10]). Nevertheless, the degree of amorphicity in the vicinity of the interfaces is a quite astonishing outcome of our simulations, since we applied (very) low temperatures in the molecular dynamics runs.

For larger gap-sizes the surfaces cannot coalesce to build common interfaces since the interaction potential between the atoms of opposite sites is too weak to cause motions which are sufficient to close the gap. Therefore, the surfaces which *per constructionem* possess dangling bonds, inhibit a rather high potential energy. To reduce these types of defects and to saturate the dangling bonds, the atoms form new rings within the respective surfaces. However, the ring sizes are variable and consequently, at the surfaces structural defects will develop. Extraordinary characteristics and most important property of the surfaces is their influence on the thermal behaviour in the structures.

The temperature development of the structures and especially in the layers of the systems is a good indicator whether a configuration has gaps confined by surfaces reducing the energy transport or builds interfaces through which the thermal/kinetic energy can be transported. A finding, which at least resembles both experimental outcomes [9] and theoretical results [2], is connected with the thermal and temperature evolution at interfaces. The generation of an interface via coalescence of two surfaces leads to a (continuous) temperature distribution through the complete system, and to a development of a standard deviation which do not differ from layers in the bulk. Such "relaxations" of the temperatures are at least in qualitative agreement with findings of experiments on thermal conductivity in hetero-structures comprising a thin film deposited on bulk material [10]. Whether the generated interface is crystalline, has defects or is disordered cannot be revealed by the temperature development.

In contrast to the interfaces the surfaces cause a totally different reaction of the systems. In the case of a simulation using constant temperature the layer at the surface developed a larger standard deviation compared to the layers in the bulk. However, the application of temperature gradients is even more strongly influenced through the gaps, and vice versa reveals the presence of surfaces. Because the energy or the temperature pulse cannot cross the surface (trapping of modes, see Ref. [1]), it is reflected by the surfaces (since our simulations are performed *in vacuo*). Therefore, and because the layer close to the surface is comprised by only few atoms (which also fluctuate) we observe a larger standard deviation of the temperature in the respective layer which consequently will correlate with the number of defects at the surface or the degree of disorder. Most important property of the temperature gradient is the development of a temperature jump due to the heat barrier which is established by the surfaces between the two sub-structures.

Appendix A. Supplementary material

Supplementary data associated with this article can be found in the online version of 10.1016/j.physb.2011.02.074.

References

[1] A.A. Balandin, J. Nanosci. Nanotechnol. 5 (2005) 1015.
[2] S. Aubry, C.J. Kimmer, A. Skye, P.K. Schelling, Phys. Rev. B 78 (2008) 064112.
[3] M.M. Hasan, Y. Zhou, H. Mahfuz, S. Jeelani, Mater. Sci. Eng. A 429 (2006) 181.

[4] S.M. Lindsay, Introduction to Nanoscience, Oxford University Press, New York, 2010.
[5] T. Okubo, A. Tsuchida, T. Kato, Colloid. Polym. Sci. 277 (1999) 191.
[6] M.A. Asoro, D. Kovar, Y. Shao-Horn, L.F. Allard, P.J. Ferreira, Nanotechnology 21 (2010) 025701.
[7] T. Hawa, M.R. Zachriah, J. Aerosol Sci. 37 (2006) 1.
[8] B.J. Henz, T. Hawa, M. Zachariah, Mol. Simulation 35 (2009) 804.
[9] L.J. Salerno, P. Kittel, NASA Technical Memorandum 110429, Thermal Contact Conductance, 1997.
[10] B. Krenzer, A. Janzen, P. Zhou, D. von der Linde, M. Horn-von Hoegen, N. J. Phys. 8 (2006) 160 see 〈http://njp.org/〉.
[11] F.J. DiSalvo, Science 285 (1999) 703.
[12] E.Y. Tsymbal, D.G. Pettifor, Solid State Physics, in: H. Ehrenreich, F. Spaepen (Eds.), Academic Press, New York, , 2001.
[13] J.K. Holt, et al., Science 312 (2006) 1034.
[14] A. Basu Mukhopadhyay, C. Oligschleger, M. Dolg, Phys. Rev. B 69 (2004) 12202.
[15] J.C. Schön, H. Putz, M. Jansen, J. Phys.: Condensed Matter 8 (1996) 143.
[16] M.A.C. Wevers, J.C. Schön, M. Jansen, J. Phys.: Condensed Matter 11 (1999) 6487.
[17] H.R. Schober, C. Gaukel, C. Oligschleger, Defect Diffusion Forum 143–147 (1997) 723.
[18] H.R. Schober, C. Gaukel, C. Oligschleger, Prog. Theor. Phys. (Kyoto) 126 (1997) 67.
[19] C. Oligschleger, C. Gaukel, H.R. Schober, J. Non-Cryst. Solids 250–252 (1999) 660.
[20] C. Oligschleger, H.R. Schober, Phys. Rev. B 59 (1999) 811.
[21] J. Reinisch, A. Heuer, Phys. Rev. Lett. 95 (2005) 155502.
[22] J. Qian, R. Hentschke, A. Heuer, J. Chem. Phys. 111 (1999) 10177.
[23] M. Lacevic, S.C. Glotzer, J. Phys. Chem. B 108 (51) (2004) 19623.
[24] M.I. Vogel, S.C. Glotzer, Phys. Rev. Lett. 92 (25) (2004) 255901.
[25] W. Kob, C. Donati, S.J. Plimpton, P.H. Poole, S.C. Glotzer, Phys. Rev. Lett. 79 (1997) 2827.
[26] M. Warren, J. Rottler, Phys. Rev. Lett. 104 (2010) 205501.
[27] W. Kob, J.-L. Barrat, Phys. Rev. Lett. 78 (1997) 45814584.
[28] H. Miyagawa, Y. Hiwatari, Phys. Rev. A 40 (1989) 6007.
[29] B.B. Laird, H.R. Schober, Phys. Rev. Lett. 66 (1991) 636.
[30] H.R. Schober, B.B. Laird, Phys. Rev. B 44 (1991) 6746.
[31] A. Tanguy, B. Mantisi, M. Tsamados, Eur. Phys. Lett. 90 (2010) 16004.
[32] T. Mues, M. Burger, I. Lubashevsky, A. Heuer, Phys. Rev. E 81 (2010) 051605.
[33] P. Hansen, I.R. McDonald, Theory of Simple Liquids, Academic, New York, 1976.
[34] G. Cicotti, D. Frenkel, I.R. McDonald (Eds.), Simulations of Liquids and Solids, North Holland, Amsterdam, 1987.
[35] M.P. Allen, D.J. Tildesley, Computer Simulation of Liquids, Oxford, Clarendon, 1987.
[36] B.J. Garrison, Chem. Soc. Rev. 155 (1992).
[37] D. LiYing, et al., Sci. China Ser. B 51 (7) (2008) 651.
[38] A. Schüring, et al., Diffusion Fundam. 6 (2007) 33.1.
[39] A. Ito, H. Nakamura, Commun. Comput. Phys. 4 (2008) 592.
[40] P. Valentini, T. Dumitrica, J. Nano Res. 1 (2008) 31.
[41] R.L. Davidchack, B.B. Laird, Mol. Phys. 97 (1999) 833.
[42] R.L. Davidchack, B.B. Laird, Phys. Rev. Lett. 85 (2000) 4751.
[43] M. Amini, B.B. Laird, Phys. Rev. Lett. 97 (2006) 216102.
[44] P. Vashishta, R.K. Kalia, J.P. Rino, I. Ebbsjö, Phys. Rev. B 41 (1990) 12197.
[45] F.H. Stillinger, T.A. Weber, R.A. La Violette, J. Chem. Phys. 85 (1986) 6460.
[46] F.H. Stillinger, T.A. Weber, J. Phys. Chem. 91 (1987) 4899.
[47] S.W. de Leeuw, J.W. Perram, E.R. Smith, Proc. R. Soc. A 373 (1980) 27.
[48] S.W. de Leeuw, J.W. Perram, E.R. Smith, Proc. R. Soc. A 373 (1980) 56.
[49] A. Nakano, L. Bi, R.K. Kalia, P. Vashishta, Phys. Rev. Lett. 71 (1993) 85.
[50] R.K. Kalia, A. Nakano, P. Vashishta, C.L. Rountree, L. van Brutzel, S. Ogata, Int. J. Frac. 121 (2003) 71.
[51] L. van Brutzel, C.L. Rountree, R.K. Kalia, A. Nakano, P. Vashishta, Mater. Res. Soc. Symp. Proc. 703 (2002) 12.
[52] M.I. Trioni, A. Bongiorno, L. Colombo, J. Non-Cryst. Solids 220 (1997) 164.
[53] D.W. Heermann, Computer Simulation Methods, Springer, Berlin, 1990.
[54] S. Nosé, M.L. Klein, Mol. Phys. 50 (1983) 1055.
[55] K. Vollmayr, W. Kob, K. Binder, Phys. Rev. B 54 (1996) 15808.
[56] D. Caprion, J. Matsui, H.R. Schober, Phys. Rev. Lett. 95 (2000) 4293.
[57] D. Caprion, H.R. Schober, Phys. Rev. B 63 (2000) 3709.
[58] J.M. Dickey, A. Paskin, Phys. Rev. 188 (1969) 1407.
[59] D. Beeman, R. Alben, Adv. Phys. 26 (1977) 339.
[60] C. Oligschleger, Phys. Rev. B 60 (1999) 3182.
[61] A. Basu Mukhopadhyay, C. Oligschleger, M. Dolg, Phys. Rev. B 68 (2003) 24205.
[62] A. Heuer, Phys. Rev. Lett. 78 (1997) 4051.
[63] A. Heuer, H.W. Spiess, Phys. Rev. Lett. 83 (1999) 1335.
[64] W. Kob, H.C. Andersen, Phys. Rev. E 51 (1995) 4626.
[65] G. Schaftenaar, J.H. Noordik, J. Comput. 14 (2000) 123.
[66] R.G.W. Wyckoff, Crystal Structures, Krieger, Florida, 1982.
[67] S.N. Taraskin, S.R. Elliott, Phys. Rev. B 58 (1997) 8605.